Nuclear Pore Complex Clustering and Nuclear Accumulation of Poly(A)$^+$ RNA Associated with Mutation of the *Saccharomyces cerevisiae RAT2 / NUP120* Gene

Catherine V. Heath,* Connie S. Copeland,‡ David C. Amberg,* Veronica Del Priore,* Michael Snyder,‡ and Charles N. Cole*

*Department of Biochemistry, Dartmouth Medical School, Hanover, New Hampshire 03755; and ‡Department of Biology, Yale University, New Haven, Connecticut 06511

Abstract. To identify genes involved in the export of messenger RNA from the nucleus to the cytoplasm, we used an in situ hybridization assay to screen temperature-sensitive strains of *Saccharomyces cerevisiae*. This identified those which accumulated poly(A)$^+$ RNA in their nuclei when shifted to the non-permissive temperature of 37°C. We describe here the properties of yeast strains carrying mutations in the *RAT2* gene (*RAT* - ribonucleic acid trafficking) and the cloning of the *RAT2* gene. Only a low percentage of cells carrying the *rat2-1* allele showed nuclear accumulation of poly(A)$^+$ RNA when cultured at 15° or 23°C, but within 4 h of a shift to the nonpermissive temperature of 37°C, poly(A)$^+$ RNA accumulated within the nuclei of approximately 80% of cells. No defect was seen in the nuclear import of a reporter protein bearing a nuclear localization signal. Nuclear pore complexes (NPCs) are distributed relatively evenly around the nuclear envelope in wild-type cells. In cells carrying either the *rat2-1* or *rat2-2* allele, NPCs were clustered together into one or a few regions of the nuclear envelope. This clustering was a constitutive property of mutant cells. NPCs remained clustered in crude nuclei isolated from mutant cells, indicating that these clusters are not able to redistribute around the nuclear envelope when nuclei are separated from cytoplasmic components. Electron microscopy revealed that these clusters were frequently found in a protuberance of the nuclear envelope and were often located close to the spindle pole body. The *RAT2* gene encodes a 120-kD protein without similarity to other known proteins. It was essential for growth only at 37°C, but the growth defect at high temperature could be suppressed by growth of mutant cells in the presence of high osmolarity media containing 1.0 M sorbitol or 0.9 M NaCl. The phenotypes seen in cells carrying a disruption of the *RAT2* gene were very similar to those seen with the *rat2-1* and *rat2-2* alleles. Epitope tagging was used to show that Rat2p is located at the nuclear periphery and co-localizes with yeast NPC proteins recognized by the RL1 monoclonal antibody. The *rat2-1* allele was synthetically lethal with both the *rat3-1/nup133-1* and *rat7-1/nup159-1* alleles. These results indicate that the product of this gene is a nucleoporin which we refer to as Rat2p/Nup120p.

NUCLEAR pore complexes (NPCs)[1] play a central role in the exchange of macromolecules between the nuclear and cytoplasmic compartments of eukaryotic cells (for reviews see Rout and Wente, 1994; Davis, 1995; Doye and Hurt, 1995). NPCs are large complex structures which perforate the nuclear envelope; they have a mass of approximately 125 million daltons in metazoan cells, 65 million daltons in yeast cells, and may contain as many as 100 distinct polypeptides (Reichelt et al., 1990; Rout and Blobel, 1993). When examined by high resolution electron microscopy, NPCs are seen to have an eightfold rotational symmetry. Three-dimensional image reconstruction suggests that NPCs contain nuclear and cytoplasmic rings with spokes radiating inwardly from these rings to define a central channel where the transporter apparatus is thought to be located (Unwin and Milligan, 1982; Akey, 1990, 1991; Reichelt et al., 1990; Jarnik and Aebi, 1991; Hinshaw et al., 1992; Akey and Radermacher, 1993). Filamentous structures have been observed projecting from NPCs into both the cytoplasm and the nucleoplasm (Maul, 1977; Richardson et al., 1988; Allen and

Address correspondence to C. N. Cole, Department of Biochemistry, Dartmouth Medical School, 7200 Vail Building/Room 413, Hanover, New Hampshire 03755. Ph.: (603) 650-1628. Fax: (603) 650-1128. E-mail: Charles.Cole@Dartmouth.edu

D. C. Amberg's present address is Department of Genetics, Stanford University Medical Center, Stanford, CA 94305.

1. *Abbreviations used in this paper*: 5-FOA, 5-fluoroorotic acid; NLS, nuclear localization signal; NPC, nuclear pore complex.

Douglas, 1989; Jarnik and Aebi, 1991; Goldberg and Allen, 1992; Ris and Malecki, 1993). The nucleoplasmic filaments are organized into a basket-like structure called the fishtrap, which may contain sites for docking of macromolecules being exported from the nucleus. In metazoan cells, NPCs appear to be physically anchored to the nuclear lamina (Stewart and Whytock, 1988; Akey, 1989). Little is known about the assembly of NPCs or their insertion into the nuclear envelope.

NPCs possess 9-nm aqueous channels that permit small molecules including ions and metabolites to cross the nuclear envelope by passive diffusion. Translocation of larger molecules across the NPC, including proteins and RNAs, is an active process that is energy dependent, saturable, and requires specific signals in the molecules being transported. Recent studies indicate that the small GTP-binding protein Ran/TC4 is one of the factors responsible for protein import in vertebrate cells (Melchior et al., 1993; Moore and Blobel, 1993; Ren et al., 1993) and that its yeast homologs, Gsp1p and Gsp2p, play a similar role in *Saccharomyces cerevisiae* (Schlenstedt et al., 1995). These proteins are also likely to be involved in export from the nucleus to the cytoplasm since accumulation of poly(A)$^+$ RNA in the nuclei of yeast cells was observed in cells carrying mutations affecting Gsp1p, or Rna1p, its GTPase activating protein Rna1p, of Prp20p, its guanine nucleotide exchange factor (Amberg et al., 1992; Forrester et al., 1992; Kadowaki et al., 1992; Amberg et al., 1993; Schlenstedt et al., 1995).

Immunological, biochemical and genetic approaches have been taken to identify nucleoporins. Isolated rat liver nuclear envelopes were used to generate monoclonal antibodies reactive with proteins associated with the nuclear envelope, and many of these antibodies recognize short repeated peptide motifs common to many nucleoporins (Davis and Blobel, 1986; Park et al., 1987; Snow et al., 1987). This has facilitated the purification of specific nucleoporins and the cloning of the genes or cDNAs encoding these proteins. Many of these antibodies to rat liver nuclear envelopes also recognize nucleoporins from *S. cerevisiae* (Aris and Blobel, 1989; Copeland and Snyder, 1993) permitting their use in cloning of yeast nucleoporins (Davis and Fink, 1990; Wente et al., 1992; Loeb et al., 1993). Other nucleoporins have been identified based on their co-purification with repeat-containing nucleoporins (Snow et al., 1987; Finlay et al., 1991; Buss and Stewart, 1995; Grandi et al., 1993, 1995*b*).

Genetic approaches in yeast have proved valuable in the identification of nucleoporins. We described a genetic approach to identify gene products important for the nucleocytoplasmic export of poly(A)$^+$ RNA in yeast (Amberg et al., 1992). We screened a bank of temperature-sensitive mutants of *S. cerevisiae* by in situ hybridization for those which accumulated poly(A)$^+$ RNA in their nuclei when shifted to the nonpermissive temperature of 37°C. This led to the identification of additional yeast nucleoporins (Gorsch et al., 1995; Li et al., 1995). Synthetic lethal genetic screens have also been a productive pathway to the identification of yeast nucleoporins (Wimmer et al., 1992; Doye et al., 1994; Fabre et al., 1994). Furthermore, the ability to purify yeast NPCs has accelerated the identification of additional *S. cerevisiae* nucleoporins (Rout and Blobel, 1993; Wozniak et al., 1994; Hurwitz and Blobel, 1995; Kraemer et al., 1995; Pemberton et al., 1995).

Three major repeat-containing classes of nucleoporins have been identified (Davis, 1995). The XFXFG class includes metazoan p62, nup153, nup214, and pom121, and the yeast nucleoporins Nup1p, Nup2p, and Nsp1p (Davis and Fink, 1990; Nehrbass et al., 1990; Loeb et al., 1993). A second class of nucleoporins contains GLFG repeats and includes p98 from rat (Radu et al., 1995), p97 from *Xenopus* (Powers et al., 1995), and Nup49p, Nup57p, Nup100p, Nup116p, and Nup145p from *S. cerevisiae* (Wente et al., 1992; Wimmer et al., 1992; Wente and Blobel, 1993; Fabre et al., 1994; Wente and Blobel, 1994; Grandi et al., 1995*b*). A third class of nucleoporins contain degenerate XXFG repeats. Within this group, yeast Rat7p/Nup159p contains 25 XXFG repeats, with SAFG and PSFG being most common (Gorsch et al., 1995). Very similar repeats are found in rat nup214 (Kraemer et al., 1994; Panté et al., 1994). To date, the only yeast nucleoporins identified that lack repeat motifs are Nic96p (Grandi et al., 1993), Rat3p/Nup133p (Doye et al., 1994; Li et al., 1995; Pemberton et al., 1995), and Nup82p (Grandi et al., 1995*a*; Hurwitz and Blobel, 1995).

We report here the identification of Rat2p/Nup120p, an additional yeast nucleoporin lacking repeat motifs. We initially isolated the *rat2-1* strain by screening UV-mutagenized yeast for strains which were temperature sensitive for growth and accumulated poly(A)$^+$ RNA in their nuclei at the nonpermissive temperature. We cloned the *RAT2* gene by complementation. It encodes a 120-kD protein which we show by indirect immunofluorescence to colocalize at the nuclear rim with known yeast NPC components. Yeast strains bearing mutant alleles of *RAT2* show constitutive clustering of NPCs. This clustering is retained in isolated crude nuclei, suggesting that connections to the cytoskeleton are not required for proper distribution of NPCs. While these strains accumulate poly(A)$^+$ RNA in their nuclei following a shift to 37°C, protein import does not appear to be affected by mutation or disruption of this gene. Mutant strains were able to grow at high temperatures (37°C) in the presence of 1 M sorbitol. Under these conditions, the block to export of poly(A)$^+$ RNA was partially suppressed but clustering of NPCs in mutant cells was retained. A modest disruption of the nucleolus was seen in mutant strains shifted to the nonpermissive temperature, but synthesis and processing of rRNA continued following the temperature shift. Synthetic lethality was seen between strains carrying mutant alleles of *RAT2/NUP120* and strains with mutations in *RAT3/NUP133* or *RAT7/NUP159*, indicating genetic interactions among these nucleoporins.

Materials and Methods

Yeast Cell Culture, Strains, Media, Mutant Isolation, and Cell Fractionation

Table I lists the yeast strains used in this work. The plasmids used are listed in Table II. *S. cerevisiae* were cultured by standard methods (Rose et al., 1989; Sherman, 1991). Wild-type strains FY23 and FY86, *GAL2*$^+$ derivatives of S288C carrying the *ura3-52* allele, were obtained from F. Winston (Harvard Medical School, Boston, MA). Strains K31-10A, containing the mutant *met14* allele, and strain JM5010, containing an integra-

Table I. Yeast Strains Used in This Study

Strains	Genotype	Source
Dat4-2	*Mata trp1Δ63 leu2Δ1 ura3-52 rat2-1*	This study
Dat3-2	*Mata ura3-52, trip1Δ63, leu2Δ1, rat3-1*	Li et al., 1995
Fy23	*Mata trp1Δ63 leu2Δ1 ura3-52*	Provided by F. Winston
FY86	*Matα his 3Δ200 leu2Δ1 ura3-52*	Provided by F. Winston
K381-10A	*Matα ura3-1 ade6 arg4 aro7-1 asp5 met14 lys2-1 pet17 trp1*	Provided by M. Brandriss
JM5010	*Matα put3-4 ::TRP1 ura3-52 trp1*	Provided by M. Brandriss
LGY101	*Matα his3Δ200 leu2Δ1 ura 3-52 rat7-1*	L.Gorsch
LGY103	*Mata trp1Δ63 leu2Δ1 ura3-52 rat7-1*	L.Gorsch
LGY105	*Mata/Matα his3Δ200/his3Δ200 leu2Δ1/leu2Δ1 ura3-52/ura3-52*	L. Gorsch
OLY101	*Matα his3Δ200 leu2Δ1 ura3-52 rat3-1*	This study
CHY101	*Mata trp1Δ63 leu2Δ1 ura3-52* pCH7 integrated at *rat2-1* locus	This study
CHY102	*Mata trp1Δ63 leu2Δ1 ura3-52* pCH7 integrated at *RAT2* locus	This study
CHY103	*Mata/Matα his3Δ200/his3Δ200 leu2Δ1/leu2Δ1 ura3-52/ura3-52 RAT2/RAT2::HIS3*	This study
CHY104	*Mata his3Δ200 leu2Δ1 ura3-52 RAT2::HIS3*	This study
CHY105	*Mata trp1Δ63 leu2Δ1 ura3-52* pCH3 *(URA3 RAT2)*	This study
CHY106	*Mata/Matα ura3-52/ura3-52 leu2Δ1/leu2Δ1 trp1Δ63/TRP1 his3Δ200/HIS3 rat2-1/RAT2 RAT3/rat3-1*	This study
CHY107	*Mata his3Δ200 leu2Δ1 ura3-52 RAT2::HIS3 pCH12(LEU2 RAT2$_{myc}$)*	This study
CCY165	*Matα ura3-52, his3Δ200, pep4::HIS3, prb1-Δ1.6R, can1, gal2*	Snyder lab strain
CCY282	*Mata trp1Δ63 leu2Δ1 ura 3-52 rat2-1* (from 3RD backcross)	This study
DAt4xt4	*Mata/Matα ura3-52/ura3-52 leu2Δ1/leu2Δ1 trp1Δ63/TRP1 his3Δ200/HIS3 rat2-1/rat2-1*	This study
DAt2xt2	*Mata/Matα ura3-52/ura3-52 leu2Δ1/leu2Δ1 trp1Δ63/TRP1his3Δ200/HIS3 rat2-2/rat2-2*	This study
DAt1xt1	*Mata/Matα ura3-52/ura3-52 leu2Δ1/leu2Δ1 trp1Δ63/TRP1his3Δ200/HIS3 rat1-1/rat1-1*	This study
LDY97	*Matα leu2-3,112 ura3-52 his3 NUP1::LEU2* (*CEN HIS3* plasmid bearing *nup1-106* allele)	Provided by L. Davis
EE1b	*Mata ura3-52 ade2-1 tyr1 gal$^-$his$^-$ rna1-1*	Provided by A. Hopper

tion of *TRP1* into the *PUT3* locus, were obtained from M. Brandriss (New Jersey Medical School, Newark, NJ). Cells containing mutant alleles of *RAT2* were usually grown at 23°C on rich medium (YPD) (Sherman, 1991). Standard methods were used for analysis of phenotypes, strain crosses, dominance/recessive tests, and dissection of tetrads. For induction of genes under control of the *GAL1* promoter, strains were grown overnight in YP-raffinose media containing 2% raffinose in place of dextrose; the *GAL1* promoter was induced by addition of galactose to a final concentration of 2%.

The isolation of *rat* mutants (*ribonucleic acid trafficking*) has been previously described (Amberg et al., 1992). Briefly a collection of 1200 temperature-sensitive strains generated by mutagenesis with ultraviolet light was screened microscopically after in situ hybridization with digoxigenin-tagged oligo-dT$_{50}$ to localize poly(A)$^+$ RNA, followed by incubation with fluoresceinated anti-digoxigenin antibodies. Strains exhibiting fluorescent signal in the nucleus following growth at 37°C were re-purified and several were chosen for further study.

For temperature-shift experiments, cells cultured in liquid media at room temperature were shifted to rotating 37°C incubators and incubation was continued as indicated in the figure legends. To prepare growth curves, single colonies of wild-type or mutant yeast cells were inoculated into 5 ml of YPD and allowed to grow overnight at room temperature. Cell density was determined with a hemacytometer. Duplicate cultures of each strain were diluted to between 4 and 8 × 10^6 cells/ml in YPD, recounted, and incubated at 23°C. After 4 h, an aliquot of each culture was removed and counted and one culture from each strain was shifted to 37°C. Duplicate samples were removed from each culture every 4 h and cell concentration determined by counting. To examine reversion, cells were removed from each culture after 28 h and plated on YPD plates. Plates were incubated at 23° or 37°C for a week and colony numbers determined daily. To study the effect of high osmolarity on the growth and properties of wild-type and various mutant strains, either NaCl or sorbitol were added to media to final concentrations of 0.9 or 1.0 M, respectively.

Isolation of a crude nuclear fraction for indirect immunofluorescence was carried out by the short protocol described by Mirzayan et al. (1992).

Cloning and Physical Mapping of the RAT2 Gene

The *RAT2* gene was cloned by complementation of the temperature-sensitive growth defect in strain DAt4-2 (*rat2-1*) by using a genomic library of

Table II. Plasmids Used in This Study

Plasmids	Markers	Comments	Source
Yeast/Bacterial Shuttle Plasmids			
pCH1	*CEN4 LEU2*	putative *RAT2* clone No.1 in p366	This study
pCH2	*CEN4 LEU2*	putative *RAT2* clone No.2 in p366	This study
pCH3	*CEN4 URA3*	gene A* (*RAT2*) in YCplac33	This study
pCH4	*CEN4 LEU2*	gene A* (*RAT2*) in YCplac111	This study
pCH5	*CEN4 LEU2*	gene B* in YCplac111	This study
pCH6	*CEN4 LEU2*	gene C* in YCplac111	This study
pCH7	*URA3*	gene A* (*RAT2*) in YIplac211	This study
pCH12	*CEN4 LEU2*	pCH10 in YCplac111	This study
pCH13	*CEN4 LEU2*	myc epitope-tagged Rat2p in pCH12	This study
pLG4	*CEN4 URA3*	*RAT7* in YCplac33	This study
Bacterial Plasmids			
pCH8	2.1-kb *Pst* I-*Pst* I fragment of pCH4 in pBlueSK+		This study
pCH9	6.1-kb *Sac* I-*Sal* I fragment of pCH4 including *RAT2* in pUC19		This study
pCH10	site-directed mutagenesis of pCH9		This study
pCH11	disruption of *RAT2* by *HIS3* in pCH4		This study

*These letters correspond to the open reading frames shown in Fig. 3 A.

S. cerevisiae DNA (*Sau* 3A partial digestion products) cloned into a *LEU2-CEN* plasmid (a gift from P. Hieter, Johns Hopkins Univ., Baltimore, MD). This library was transformed into the mutant strain by electroporation and *LEU*$^+$ colonies were selected at 37°C. Plasmid DNA was isolated from these strains (Rose et al., 1989), transformed into *Escherichia coli*, and plasmids isolated for further analyses. Plasmids were tested for their ability to re-transform the mutant strain to *LEU*$^+$ and growth at 37°C. All plasmids able to transform the strain contained overlapping yeast DNA segments. Different plasmid clones overlapped by ~7.2 kb. Subclones containing a 6.1-kb SacI-SalI fragment of pCH2 complemented both the temperature sensitivity as well as the aberrant RNA localization phenotype of the *rat2-1* strain.

A 1.0-kb DraI fragment common to all complementing plasmids was used to probe a blot of electrophoretically separated yeast chromosomes and a set of ordered cosmids and lambda phages containing almost the entire yeast genome (Riles et al., 1993). The chromosome blot indicated that the *RAT2* gene is located on chromosome XI. The same probe identified a single lambda clone located ~40 cM from the centromere on the left arm of chromosome XI. This physical position of the cloned DNA agreed with genetic mapping data (see below).

Disruption of the RAT2 Gene

To disrupt the *RAT2* gene, the entire *RAT2* open reading frame except for the first 86 and last 60 amino acids was replaced with the *HIS3* gene. pCH4, containing the complete *RAT2* open reading frame, was digested with NcoI and PstI, and a 7.2-kb fragment was isolated after electrophoresis on a 0.8% agarose gel in TBE buffer. This fragment was eluted and ligated with a 1,068-bp *Eco47* III-NsiI DNA fragment of plasmid pRS403 (Stratagene Inc., La Jolla, CA) containing the complete *HIS3* gene. This resulting plasmid, pCH11, was digested with SphI and XmaI to release a fragment containing *RAT2* sequences flanking the inserted *HIS3* gene. Diploid wild-type cells (strain LGY105) were transformed with this fragment by electroporation and colonies able to grow on SC-HIS media were selected. Southern analysis was used to show that the fragment had integrated into the *RAT2* locus (data not shown). The resulting strain was transformed with plasmid pCH3 which contains the complete *RAT2* gene and the *URA3* gene in YCplac33. After sporulation, tetrads were dissected and allowed to germinate on rich media at 23°C. Cells were then replica plated to SC-HIS plates containing 5-fluoroorotic acid (5-FOA) and the plates were incubated at both 23° and 37°C.

Integration of an Auxotrophic Marker Adjacent to RAT2 and Genetic Mapping of RAT2

A 3.3-kb fragment containing part of the *RAT2* gene was isolated after digestion of pCH1 and ligated into the polylinker region of KpnI-digested YIPlac211 to create pCH7. This plasmid was linearized by digestion with ClaI, which cleaves within *RAT2* sequences, and transformed by electroporation into wild-type strain FY86 and into YCC282 carrying the *rat2-1* allele. Cells were plated and grown on SC-URA plates for 4 d. Colonies were picked, and the appropriate integration pattern was confirmed by Southern blotting using an ECL kit. The resulting strains, named CHY102 (integration into the wild-type FY86 strain) and CHY101 (integration into the *rat2-1* strain), were mated with strains CCY282 and FY86, respectively. Diploids were grown in sporulation media for 7–14 d. Tetrads were dissected and the genotypes of the haploids tested.

A haploid strain bearing the *rat2-1* allele (CCY282) was crossed with: (*a*) a strain (K31-10A) that was unable to grow without added methionine due to a mutation in *met14*, which is located 1.7 cM from the centromere on the right arm of chromosome XI (Brandriss, 1987; Mortimer et al., 1992); and (*b*) a strain (JM5010) which contains the *TRP1* gene inserted into the *PUT3* gene, which is located 6 cM from the centromere on the left arm of chromosome XI (Brandriss, 1987). After diploids were sporulated, tetrads were dissected, and scored for segregation of the temperature sensitive *rat2-1* phenotype and for either methionine auxotrophy (associated with *met14*) or tryptophan prototrophy (associated with the *PUT3*::*TRP1* locus). For the cross of the *rat2-1* strain with the *met14* strain, temperature-sensitivity and methionine prototrophy segregated 3:0:9 (parental ditypes/non-parental ditypes/tetratypes). For the cross of the *rat2-1* strain with the *PUT3*::*TRP1* strain, the data were 19:2:24 (PD:NPD:TT). The data indicate that *RAT2* is located approximately 54 cM from *MET14* and 40 cM from *PUT3*.

To provide further confirmation that the cloned DNA contains *RAT2*, a 3.3-kb KpnI DNA fragment from pCH1 was cloned into the polylinker region of YIPlac211 to create pCH7. The plasmid was linearized with ClaI, which digests within the KpnI fragment, and electroporated into a wild-type strain (FY86) and colonies able to grow on SC-URA were selected. This procedure directs integration of the plasmid to the site on chromosome XI from which the cloned DNA was derived. DNA was isolated from colonies and Southern blotting was performed to confirm that the DNA from the linearized plasmid had integrated at the appropriate site (data not shown). The resulting strain, CHY102 (integration into the *RAT2* locus of the wild-type FY86 strain) was mated with strain CCY282 (*rat2-1*). Diploids were selected and transferred to sporulation media for 7–14 d. Tetrads were dissected and analyzed for the pattern of segregation of temperature sensitivity and uracil auxotrophy. All 25 four-spore tetrads analyzed were parental ditypes; uracil prototrophy and temperature sensitivity did not co-segregate in any of the tetrads.

In Situ Hybridization and Indirect Immunofluorescence

The procedure for in situ hybridization has been described (Amberg et al., 1992; Gorsch et al., 1995). The probe used to detect poly(A)$^+$ RNA was oligo(dT)$_{50}$ to which 1-4 digoxigenin-dUDP molecules were added at the 3′ end by using terminal deoxynucleotidtyl transferase. DAPI (4′, 6-diamidino-2-phenylindole-dihydrochloride) or Hoechst 33258, DNA-binding dyes, were used to stain the nuclear region of cells. We showed previously that in situ hybridization with this digoxigenin-tagged oligo-dT$_{50}$ probe detects poly(A)$^+$ RNA (Amberg et al., 1992). The fluorescent signal could be competed away with a 1,000-fold excess of untagged oligo-dT$_{50}$, but not with the same level of an unrelated oligonucleotide. The signal was also sensitive to digestion with ribonuclease and was dependent on transcription by RNA polymerase II (Amberg et al., 1992).

Indirect immunofluorescence on fixed yeast cells was performed as previously described (Mirzayan et al., 1992; Copeland and Snyder, 1993). The following antibodies were used for these analyses: Polyclonal anti-Rat7p/Nup159p antibody (Gorsch et al., 1995), reactive with GST-Rat7p/Nup159p, was produced by injection of GST-Rat7p fusion protein containing most of the repeat region of Rat7p/Nup159p into guinea pigs; monoclonal antibody RL1 (Snow et al., 1987), a mouse IgM which recognizes multiple nuclear pore proteins in both mammalian cells and in yeast, was generously provided by Dr. Larry Gerace (Scripps Research Institute, La Jolla, CA); monoclonal antibody A66 (Aris and Blobel, 1988), which recognizes the yeast nucleolar protein Nop1p, was a generous gift from Dr. John Aris (University of Florida, Gainesville, FL); monoclonal antibody 2.3B also recognizes the yeast nucleolus (Copeland, C. S., H. Friedman and M. Snyder, unpublished results). Anti-tubulin antibody YOL1/34 was obtained from Accurate Chemical and Scientific, Corp. (Westbury, NY) and detected with a FITC-conjugated goat anti-rat immunoglobulin secondary antibody (Jackson Immunoresearch, West Grove, PA). Secondary antibodies for use with mouse monoclonal antibodies included donkey anti-mouse antibodies tagged with CY3 or FITC and obtained from Jackson Immunoresearch, Inc., horse anti-mouse IgG conjugated with FITC obtained from Vector Laboratories, Inc., (Burlingame, CA) and goat anti-mouse IgM conjugated with Texas red and obtained from Vector Laboratories. The secondary antibody used with the anti-Rat7p/Nup159p antibody was an FITC-conjugated goat anti-guinea pig IgG (Vector Laboratories). The anti-Rat7p/Nup159p antibody recognizes a single polypeptide on Western blots that has been shown to be Rat7p/Nup159p (Gorsch et al., 1995) and shows a punctate rim staining pattern that is co-extensive with the RL1 staining pattern.

Indirect immunofluorescence was also performed to detect the subcellular distribution of a fusion protein consisting of the first 33 amino acids of yeast histone H2B (containing its nuclear localization signal) fused to *E. coli* β-galactosidase, and under the control of a modified *GAL1* promoter (Moreland et al., 1987). Strains were transformed with pP_{GAL}H2B-NLS-lacZ, the plasmid encoding this reporter protein. Stationary phase cultures of yeast cells were diluted 1:50 and grown overnight at 23°C in SC-URA medium containing 2% raffinose. The next morning, aliquots of each culture were shifted to 36°C for 2.5 h and then galactose was added to all cultures to a final concentration of 2%. Incubation was continued an additional 1.5 h before cells were fixed. Indirect immunofluorescence was performed using a mouse monoclonal antibody to *E. coli* β-galactosidase (Sigma Chemical Co., St. Louis, MO) diluted 1:2,000. The secondary antibody, FITC-conjugated horse anti-mouse IgG (Vector Labs, Burlingame, CA), was used at a 1:650 dilution.

Electron Microscopy

Electron microscopy was performed by a modification of published proce-

dures (Byers and Goetsch, 1975). Cells were cultured at 23°C in YPD to a density of 0.2–2 × 10^7cells/ml, harvested by filtration, fixed for 2 h at room temperature in 3% (vol/vol) glutaraldehyde containing 0.1% tannic acid in 0.1 M sodium cacodylate, pH 6.8. Fixed cells were washed twice in 50 mM KH_2PO_4/K_2HPO_4, pH 7.5, and then digested with 125 mg/ml Zymolyase 100T (ICN Immunochemicals, Irvine, CA) in 50 mM KH_2PO_4/K_2HPO_4, pH 7.5, for 40 min at 30°C. After two washes in 0.1 M sodium cacodylate, pH 6.8, the spheroplasted cells were treated with 2% (vol/vol) OsO_4 in 0.1 M sodium cacodylate, pH 6.8, for 1 h on ice. Samples were washed and stored overnight at 4°C in 0.1 M sodium cacodylate, pH 6.8. Samples were next washed three times in ddH_2O and treated for 1 h with 2% uranyl acetate in ddH_2O. After two washes in ddH_2O, cells were embedded in 2% agar, dehydrated through graded ethanol, and embedded in Spurr's medium. Thin sections were cut, stained with uranyl acetate and Reynold's lead citrate, and examined on a JEOL 100CX electron microscope at 60 kV accelerating voltage.

Epitope Tagging and Immunolocalization

Site-directed mutagenesis was used to create a unique site near the COOH terminus of the *RAT2* gene where the sequence encoding three copies of the epitope recognized by the 9E10 anti-*myc* monoclonal antibody (EQKLISEEDLN) was inserted in frame with the *RAT2* coding region. A 6.1-kb SacI-SalI fragment of pCH4 including *RAT2* was inserted into the multicloning site of pUC19. The resulting plasmid pCH9 was used as the template for the site-directed mutagenesis using a kit obtained from Clonetech Laboratories, Inc. (Palo Alto, CA). A 28-bp oligonucleotide (CTTTAACTGATTCTAGAGATGAGTTACG) containing a single nucleotide mutation was used to direct the insertion to a site 24 nucleotides from the start of the coding region of the *RAT2* gene, yielding a plasmid (pCH9) with a unique XbaI site at that position. Digestion of the plasmid pKK-1 (obtained from G. Fink, Whitehead Institute, Cambridge, MA) with XbaI yielded a 120-bp cassette containing a triplicate of the epitope recognized by the 9E10 monoclonal antibody. This was gel purified on a 0.8% agarose gel and ligated into pCH9 which had been digested with XbaI, yielding pCH10. Insertion and orientation were confirmed by restriction endonuclease digestion patterns. The resulting plasmid (pCH13) was transformed into strain CHY104, carrying the *rat2Δ* allele, yielding strain CHY107. Cells were grown to early log phase and fixed with 1/10 volume of 37% formaldehyde for 1 h. Cells were then washed three times with 1.2 M sorbitol; 50 mM K_2HPO_4, pH7.5 (solution A), resuspended into 1 ml of solution A containing 30 mg of 100T Zymolyase (Seikagaku, Rockville, MD), and incubated at room temperature for 10–60 min until spheroplasts were formed. Spheroplasts were washed once with solution A and adhered to polylysine-coated 12-well slides. Samples were washed sequentially with PBS + 0.1% BSA (solution B), solution B + 0.1% NP-40, and solution B, with a 5-min incubation per wash. Cells were incubated with the 9E10 mouse IgG monoclonal anti-*myc* antibody in solution B overnight at 4°C. Cells were then washed with solution B, solution B plus 0.1% NP-40, and solution B, each for 5 min. Cells were incubated with secondary antibody (FITC-conjugated goat anti-mouse IgG) in solution B for 2 h at room temperature and then washed with solution B, solution B plus 0.1% NP-40, and containing 10 mg of DAPI per ml, and solution B, each for 5 min. Cells were mounted with mounting solution (70% glycerol/30% PBS containing 1 mg *p*-phenylenediamine per ml). Hybridoma cells producing the 9E10 antibody were a generous gift of Drs. J. Zhu and J. M. Bishop (University of California, San Francisco, CA).

To examine the co-localization of Rat2p and nuclear pore complexes, cells were doubly stained with both the anti-*myc* epitope monoclonal antibody and with the RL1 anti-nucleoporin monoclonal antibody. The anti-*myc* antibody is an IgG while the RL1 antibody is an IgM. Secondary antibodies, horse anti-mouse IgG coupled to FITC and goat anti-mouse IgM coupled to Texas red (both from Vector Laboratories) were used at 1:500 and 1:650 dilution, respectively. Control experiments indicated that there was no detectable signal in the Texas red channel when both primary antibodies and the FITC-conjugated secondary antibody were used; similarly, there was no detectable signal in the FITC channel when both primary antibodies and only the Texas red–conjugated secondary antibody were used (data not shown).

Analysis of Pre-rRNA Processing by Pulse Labeling

All strains to be used that were *ura3*− were made URA3$^+$ by transformation with YCPlac33 (Gietz and Sugino, 1988), which contains the *URA3* gene. Cells were grown to early to mid-log phase (A_{600} of 0.3 to 0.5) in SC-Ura. 1.6 ml of cells were labeled with 160 mCi of [5-^{3}H]uridine (New England Nuclear, Boston, MA; 22 Ci/mmol) for 10 min. 30 s before the end of the labeling period, cells were collected by microcentrifugation for 20 s, the supernatant was aspirated, and the cells were quickly frozen in a dry ice/ethanol bath. Total RNA was extracted by the method of Tollervey (Tollervey and Mattaj, 1987). Briefly, to the pelleted cells were added 50 ml of 4 M guanidinium thiocyanate, 50 ml of phenol, 5 mg of tRNA and 100 ml of glass beads. Tubes were vortexed in a cold room. Then 300 ml of phenol, 300 ml of 4 M guanidinium thiocyanate were added and the mixture incubated at 65°C for 5 min. 300 ml of chloroform and 160 ml of 3 M sodium acetate were added. The mixture was centrifuged for 2 min in a microcentrifuge and the upper layer was transferred to a new tube. Extraction was repeated twice with phenol and chloroform. RNA was precipitated with ethanol and resuspended in RNase-free water. Samples were electrophoresed on a 1.2% agarose/6M formaldehyde gel. The RNA was Northern blotted to a nylon membrane (Hybond-N +; Amersham Chemical Corp., Arlington Heights, IL) which was sprayed with EN^{3}HANCE (New England Nuclear, Boston, MA) and exposed to Kodak XAR film.

Synthetic Lethality

Diploids containing both the *rat2-1* and *rat3-1* alleles were obtained by mating strains CCY282 and OLY101 with selection for diploids on SD + Leu plates. Diploids were transformed with a *URA3*-marked plasmid containing the wild-type *RAT2* gene (pCH3). Diploids containing the *rat2-1* and the *rat7-1/nup159-1* alleles were obtained by mating strains CCY282 and LGY101 and were transformed with pLG4, a *CEN* plasmid containing the *URA3* gene and the wild-type *RAT7/NUP159* gene under control of its own promoter. Diploids were sporulated and viable spores allowed to germinate after tetrad dissection. Viable spores were tested for their ability to grow in the absence of the plasmid-borne *RAT2* or *RAT7* gene by plating on media containing 5-FOA at 23°C, as well as for their ability to grow on YPD at 37°C. Of the 20, 4 spore tetrads analyzed following sporulation of the strain heterozygous for *rat2-1* and *rat3-1/nup133-1*, the ratio of those yielding 2, 3, or 4 haploids able to grow on 5-FOA plates was 3:13:4. From the tetrads yielding two haploids able to grow on 5-FOA plates, both of the strains able to grow were not temperature sensitive. From the tetrads yielding three haploids able to grow on 5-FOA plates, two of the strains were temperature sensitive and one was not. Of the tetrads yielding four haploids able to grow on 5-FOA plates, all four were temperature sensitive. Only five four-spore tetrads were obtained from the diploid heterozygous for *rat2-1* and *rat7-1/nup159-1*. All four yielded three viable haploids when plated on 5-FOA.

Results

Nuclear Accumulation of Poly(A)$^+$ RNA Occurs in Cells Carrying Mutant Alleles of RAT2 following a Shift to the Nonpermissive Temperature

A collection 1,200 *S. cerevisiae* temperature-sensitive mutants was screened to identify strains which accumulated poly(A)$^+$ RNA in their nuclei. Growing cells were shifted to the nonpermissive temperature (37°C) for 2 h and examined by in situ hybridization with a digoxigenin-labeled oligo(dT)$_{50}$ probe. An FITC-tagged anti-digoxigenin antibody was used to permit visualization of sites to which the oligo-dT$_{50}$ hybridized. Based on the initial screening, approximately 30 strains were selected for further study. These strains fall into at least 10 complementation groups. We described previously the identification and characterization of *RAT1/XRN2/HKE1* (Amberg et al., 1992), encoding an exoribonuclease, and *RAT7/NUP159* (Gorsch et al., 1995) and *RAT3/NUP133* (Li et al., 1995), encoding nucleoporins. Among the strains identified, six fell into the *RAT2* complementation group. The *rat2-1* and *rat2-2* alleles were used for the analyses presented below.

The RNA localization patterns observed in a wild-type (FY23) and a *rat2-1* strain (CCY282) are shown in Fig. 1. The top row of photographs shows the distribution of

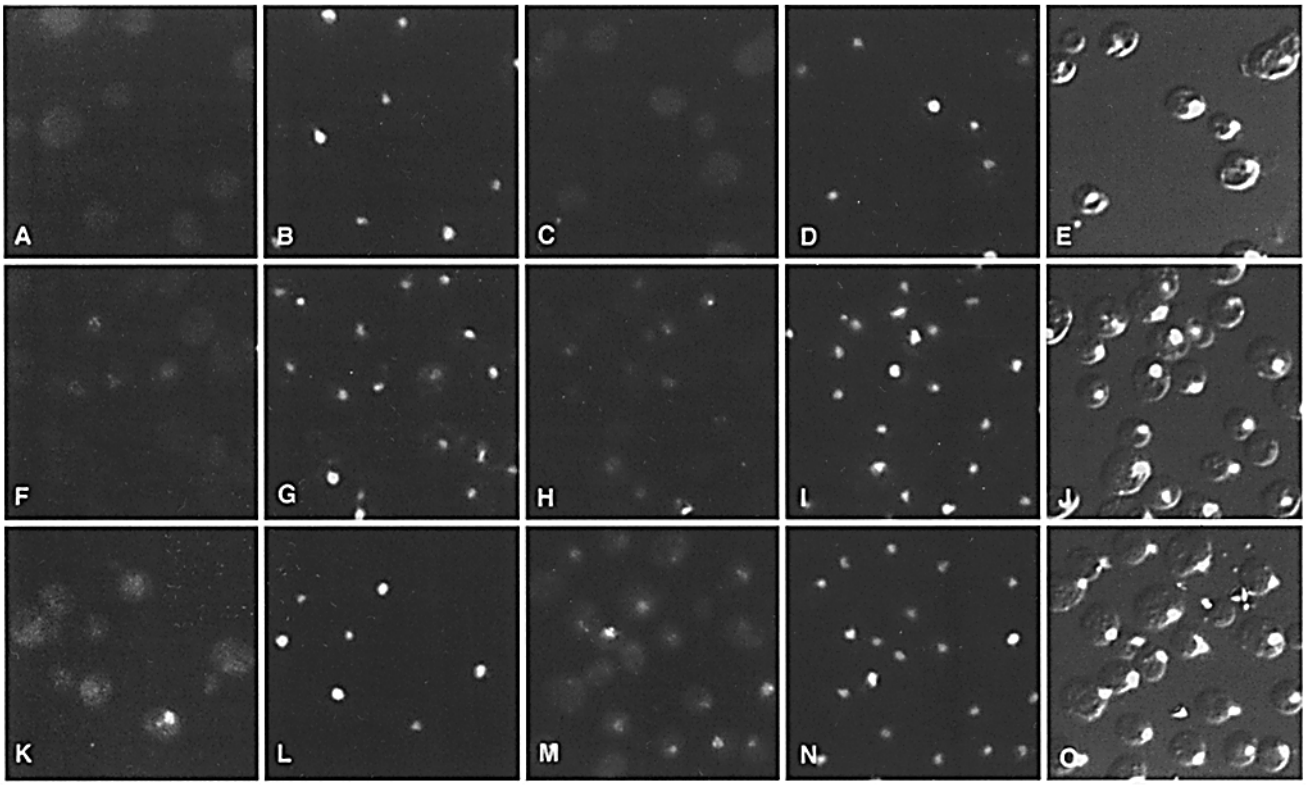

Figure 1. Accumulation of poly(A)$^+$ RNA in the nuclei of *rat2-1* and *rat2Δ* cells following a shift to 37°C. Wild-type (FY23) (*A–E*), *rat2-1* (CCY282) (*F–J*), and *rat2Δ* cells (CHY104) (*K–O*) were grown to early log phase in YPD at 23°C. Aliquots either held at 23°C (*A*, *B*, *F*, *G*, *K*, and *L*) or shifted to 37°C (*C*, *D*, *E*, *H*, *I*, *J*, *M*, *N*, and *O*) for 4 h were fixed and analyzed by an in situ hybridization assay using a digoxigenin-tagged oligo(dT)$_{50}$ probe. Sites where probe had hybridized were visualized by using a FITC-conjugated anti–digoxigenin antibody. (*A*) WT, 23°C, FITC; (*B*) same field of cells as in *A*, stained with DAPI; (*C*) WT, 37°C, FITC; (*D*) same field of cells as in *C*, stained with DAPI; (*E*) same field of cells as in *C*, stained with DAPI and simultaneously viewed by low illumination DIC microscopy; (*F*) *rat2-1*, 23°C, FITC; (*G*) same field of cells as in *F*, stained with DAPI; (*H*) *rat2-1*, 37°C, FITC; (*I*) same field of cells as in *H*, stained with DAPI; (*J*) same field of cells as in *H*, stained with DAPI and simultaneously viewed by low illumination DIC microscopy; (*K*), *rat2Δ*, 23°C, FITC; (*L*) same field of cells as in *K*, stained with DAPI; (*M*) *rat2Δ*, 37°C, FITC; (*N*) same field of cells as in *M*, stained with DAPI; (*O*) same field of cells as in *M*, stained with DAPI and simultaneously viewed by low illumination DIC microscopy.

poly(A)$^+$ RNA in wild-type cells grown continuously at 23°C (Fig. 1 *A*) or shifted to 37°C for 4 h (Fig. 1 *C*). Under both conditions, RNA was distributed throughout the cell. In contrast, poly(A)$^+$ RNA accumulated in approximately 15–20% of the nuclei of *rat2-1* cells grown at 23°C (Fig. 1 *F*). All cells also showed staining for cytoplasmic poly(A)$^+$ RNA, indicating that RNA export was occurring even though some nuclear accumulation of poly(A)$^+$ RNA was detectable. When the *rat2-1* culture was shifted to 37°C (Fig. 1 *H*), the percentage of cells showing nuclear accumulation of poly(A)$^+$ RNA increased gradually and reached a plateau of ~70–80% after 3–4 h. The signal over the cytoplasmic region was reduced, consistent with turnover of cytoplasmic RNA and reduced export from the nucleus. Even when shifted to 37°C for periods up to 12 h, the percentage of cells accumulating poly(A)$^+$ RNA in their nuclei did not increase further (data not shown).

Mutation of the RAT2 Gene Does Not Affect Nuclear Protein Import

To determine whether mutation of the *RAT2* gene also caused defects in nuclear protein import, we examined the subcellular distribution of a fusion protein containing the nuclear localization signal (NLS) of the yeast histone H2B protein fused to *E. coli* β-galactosidase (Moreland et al., 1987) and expressed from the *GAL1* promoter. We used a yeast strain carrying the *nup1-106* allele as a positive control since these cells are known to be defective for nuclear protein import (Bogerd et al., 1994). Cultures growing exponentially in YP-raffinose media were either maintained at 23°C or shifted to 36°C. We used 36°C as a non-permissive temperature because the *GAL1* promoter is more efficiently induced at 36°C than at 37°C (Gorsch, L. C., and C. N. Cole, unpublished results). Following incubation at 36°C for 2.5 h, the synthesis of the NLS-bearing reporter protein was induced by addition of galactose. Incubation was continued an additional 1.5 h before cells were fixed and processed for indirect immunofluorescence.

In wild-type cells, the fusion protein was found solely in the nucleus, regardless of whether cells were grown at 23°C (Fig. 2 *A*) or shifted to 36°C (Fig. 2 *C*). In *nup1-106* cells, fusion protein was found primarily in the nucleus in the culture maintained at 23°C (Fig. 2 *F*), but there was dramatic accumulation of the NLS-lacZ reporter protein in the cytoplasm of *nup1-106* cells shifted to 36°C for 4 h (Fig. 2 *H*). In *rat2-1* cells maintained at 23°C (Fig. 2 *K*) or shifted to 36°C for 4 h (Fig. 2 *M*), the fusion protein was

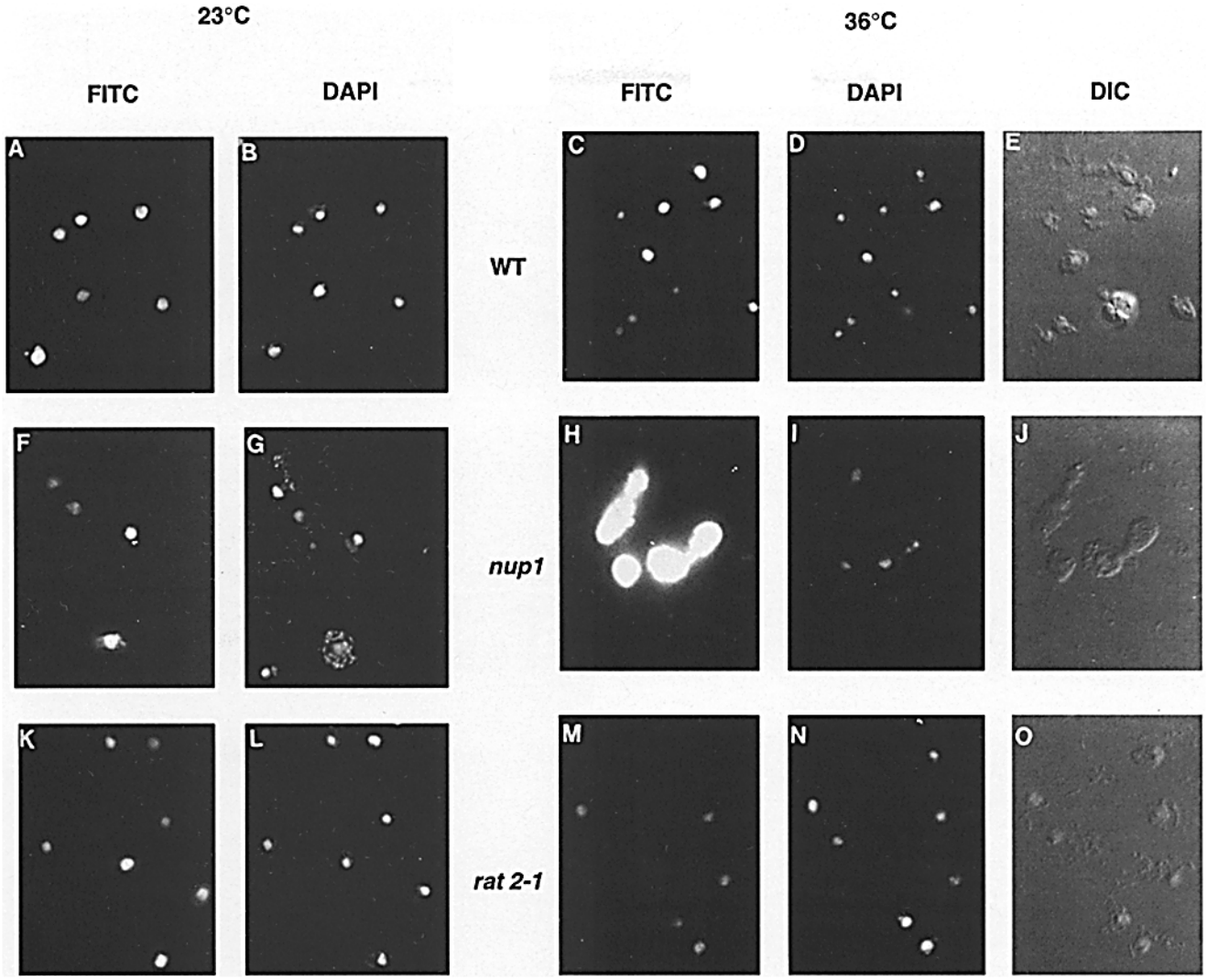

Figure 2. Normal import of a nuclear protein in a *rat2* mutant strain. Wild-type (FY23) (*A-E*), nup1 (LDY97) (*F–J*), and *rat2-1* cells (CCY282) (*K–O*) were either incubated continuously at 23°C (*A, B, F, G, K,* and *L*) or shifted to 36°C (*C, D, E, H, I, J, M, N,* and *O*) for 2.5 h before addition of galactose (to 2% final concentration) to induce expression of the reporter protein consisting of the histone H2B nuclear localization signal fused to *E. coli* β-galactosidase. After addition of galactose, incubation was continued for an additional 1.5 h before cells were fixed and processed for indirect immunofluorescence. (*A*) WT, 23°C, FITC; (*B*) same field of cells as in *A*, stained with DAPI; (*C*) WT, 36°C, FITC; (*D*) same field of cells as in *C*, stained with DAPI; (*E*) same field of cells as in *C*, viewed by DIC microscopy; (*F*) *nup1*, 23°C, FITC; (*G*) same field of cells as in *F*, stained with DAPI; (*H*) *nup1*, 36°C, FITC; (*I*) same field of cells as in *H*, stained with DAPI; (*J*) same field of cells as in *H*, viewed by DIC microscopy; (*K*) *rat2-1*, 23°C, FITC; (*L*) same field of cells as in *K*, stained with DAPI; (*M*) *rat2-1*, 36°C, FITC; (*N*) same field of cells as in *M*, stained with DAPI; (*O*) same field of cells as in *M*, viewed by DIC microscopy.

detected solely in the nucleus. Production of the fusion occurred only during the last 90 minutes of incubation at the non-permissive temperature. We conclude that the *rat2-1* mutation has little, if any, effect on nuclear protein import.

Genetic Analysis of the rat2-1 Mutation

We determined that defects in a single gene, *RAT2*, accounted for all three phenotypes observed: temperature-sensitivity, nuclear accumulation of poly(A)$^+$ RNA and nuclear pore complex clustering (see below). Haploid cells bearing the *rat2-1* allele were mated with wild-type cells, and diploids were selected, sporulated and subjected to tetrad analysis. For each allele, at least 40 tetrads were examined and found to show 2:2 segregation of temperature-sensitivity clearly implicating a single gene as the cause. Ten tetrads, including five from the third backcross were examined for co-segregation of temperature sensitivity and the RNA export phenotypes. In all cases, co-segregation and 2:2 segregation was observed. Analyses of heterozygous diploids indicated that the phenotypes of temperature sensitivity and nuclear poly(A)$^+$ RNA accumulation were recessive.

Cloning and Mapping of RAT2

The *RAT2* gene was cloned by complementation of the temperature-sensitive growth defect caused by the *rat2-1*

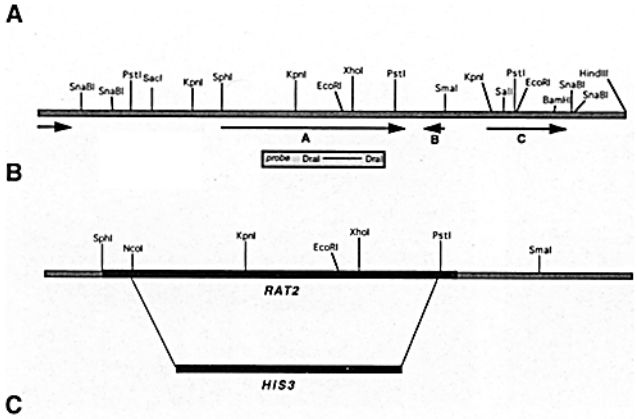

C

```
   1 MACLSRIDAN LLQYYEKPEP NNTVDLYVSN NSNNNGLKEG DKSISTPVPQ PYGSEYSNCL
  61 LLSNSEYICY HFSSRSTLLT FYPLSDAYHG KTINIHLPNA SMNQRYTLTI QEVEQQLLVN
 121 VILKDGSFLT LQLPLSFLFS SANTLNGEWF HLQNPYDFTV RVPHFLFYVS PQFSVVFLED
 181 GGLLGLKKVD GVHYEPLLFN DNSYLKSLTR FFSRSSKSDY DSVISCKLFH ERYLIVLTQN
 241 CHLKIWDLTS FTLIQDYDMV SQSDSDPSHF RKVEAVGEYL SLYNNTLVTL LPLENGLFQM
 301 GTLLVDSSGI LTYTFQNNIP TNLSASAIWS IVDLVLTRPL ELNVEASYLN LIVLWKSGTA
 361 SKLQILNVND ESFKNYEWIE SVNKSLVDLQ SEHDLDIVTK TGDVERGFCN LKSRYGTQIF
 421 ERAQQILSEN KIIMAHNEDE EYLANLETIL RDVKTAFNEA SSITLYGDEI ILVNCFQPYN
 481 HSLYKLNTTV ENWFYNMHSE TDGSELFKYL RTLNGFASTL SNDVLRSISK KFLDIITGEL
 541 PDSMTTVEKF TDIFKNCLEN QFEITNLKIL FDELNSFDIP VVLNDLINNQ MKPGIFWKKD
 601 FISAIKFDGF TSIISLESLH QLLSIHYRIT LQVLLTFVLF DLDTEIFGQH ISTLLDLHYK
 661 QFLLLNLYRQ DKCLLAEVLL KDSSEFSFGV KFFNYGQLIA YIDSLNSNVY NASITENSFF
 721 MTFFRSYIIE NTSHKNIRFF LENVECPFYL RHNEVQEFMF AMTLFSCGNF DQSYEIFQLH
 781 DYPEAINDKL PTFLEDLKSE NYHGDSIWKD LLCTFTVPYR HSAFYYQLSL LFDRNNSQEF
 841 ALKCISKSAE YSLKEIQIEE LQDFKEKQHI HYLNLLIHFR MFEEVLDVLR LGHECLSDTV
 901 RTNFLQLLLQ EDIYSRDFFS TLLRLCNAHS DNGELYLRTV DIKIVDSILS QNLRSGDWEC
 961 FKKLYCFRML NKSERAAAEV LYQYILMQAD LDVIRKRKCY LMVINVLSSF DSAYDQWILN
1021 GSKVVTLTDL RDELRGL*
```

Figure 3. The *RAT2* gene. (*A*) Schematic representation of the region of yeast chromosome XI which includes the *RAT2* gene. Key restriction endonuclease cleavage sites are shown. The arrows show three putative ORFs in this region. Also shown is the location of the DraI fragment common to all complementing plasmids and used to probe a blot of electrophoretically separated yeast chromosomes and a set of ordered cosmids and lambda phages. (*B*) Strategy for the *RAT2* disruption. The region of the gene deleted and replaced with *HIS3* to make the RAT2:: HIS3 null mutation is indicated. 86% of the*RAT2* ORF (from amino acids 86–977) was deleted by digestion with NcoI and PstI, followed by insertion of a DNA fragment containing the *HIS3* gene. (*C*) The predicted 1,037–amino acid sequence of Rat2p. These sequence data are available from Genbank/EMBL/DDBJ under accession number Z28057.

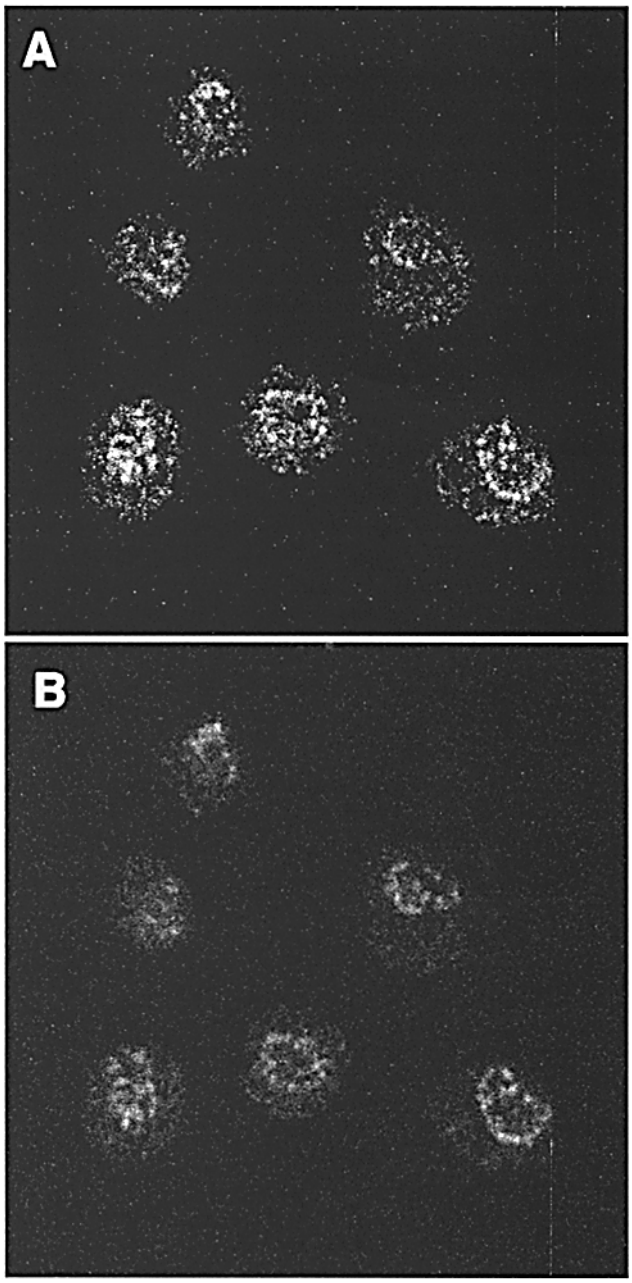

Figure 4. Rat2p is a nucleoporin. Immunolocalization of *myc*-epitope–tagged Rat2p was used to determine the subcellular location of Rat2p. Cells carrying a disruption of *RAT2* (CHY104) were transformed with a plasmid (pCH13) encoding a *myc*-epitope–tagged RAT2p, yielding strain CHY107. Cells were grown to early log phase, fixed, and processed for indirect immunofluorescence (*IF*) microscopy. (*A*) IF with anti-*myc* monoclonal antibody 9E10 and a FITC-conjugated secondary antibody. (*B*) The same field of cells as in *A*, stained with the RL1 anti-nucleoporin monoclonal antibody and a Texas red–conjugated secondary antibody.

mutation. All four distinct plasmids obtained following transformation of the *rat2-1* strain with a yeast genomic library carried on a *CEN* plasmid contained overlapping DNA fragments. A fragment derived from the region of overlap was used to probe a blot of electrophoretically separated yeast chromosomes. This indicated that the cloned DNA was derived from chromosome XI (data not shown). The same fragment was used to probe a blot containing DNA from cosmids and phages which contain ordered fragments of yeast DNA (Riles et al., 1993). This analysis confirmed that the cloned DNA was derived from chromosome XI and placed the cloned DNA near the *MET14* and *PUT3* genes. Genetic mapping experiments with a *met14* strain and with a strain containing a *TRP1* gene integrated at the *PUT3* locus indicated that *rat2-1* mutation was located ~40 cM from *PUT3* and 54 cM from *MET14*. Finally, we integrated a *URA3* marker adjacent to the *RAT2* locus in a wild-type strain and mated it with a strain carrying the *rat2-1* allele. In all haploids which arose following sporulation, the temperature sensitivity conferred by the *rat2-1* mutation segregated from the uracil prototrophy conferred by the *URA3* gene. This indicates that the *RAT2* gene, not a suppressor of the *rat2-1* mutation, is contained on the yeast DNA fragment cloned by complementation.

Based on its chromosomal position, the DNA sequence from the *MET14/PUT3* region of chromosome XI was ob-

tained from Drs. S. Rasmussen and D. von Wettstein (Carlsberg Laboratory, Copenhagen, Denmark) (Rasmussen, 1994). The smallest complementing clone was found to contain three new open reading frames (Fig. 3 *A*). Each open reading frame was subcloned into YCplac33 or YCplac111; the subclone containing the SacI to SalI DNA fragment was able to complement the *rat2-1* growth defect at 37°C and the nuclear poly(A)$^+$ RNA accumulation defect. This subclone contains a single open reading frame encoding a protein of 1,037 amino acids with a predicted size of 120 kD. The sequence of this protein is shown in Fig. 3 *C*. Rat2p lacks obvious structural features and motifs but is predicted to have a modest potential to form coiled coil interactions through amino acids 427–465 (Lupas et al., 1991). This open reading frame is designated YKL057C in the published sequences of yeast chromosome XI (Dujon et al., 1994).

To determine whether the *RAT2* gene is essential, all of

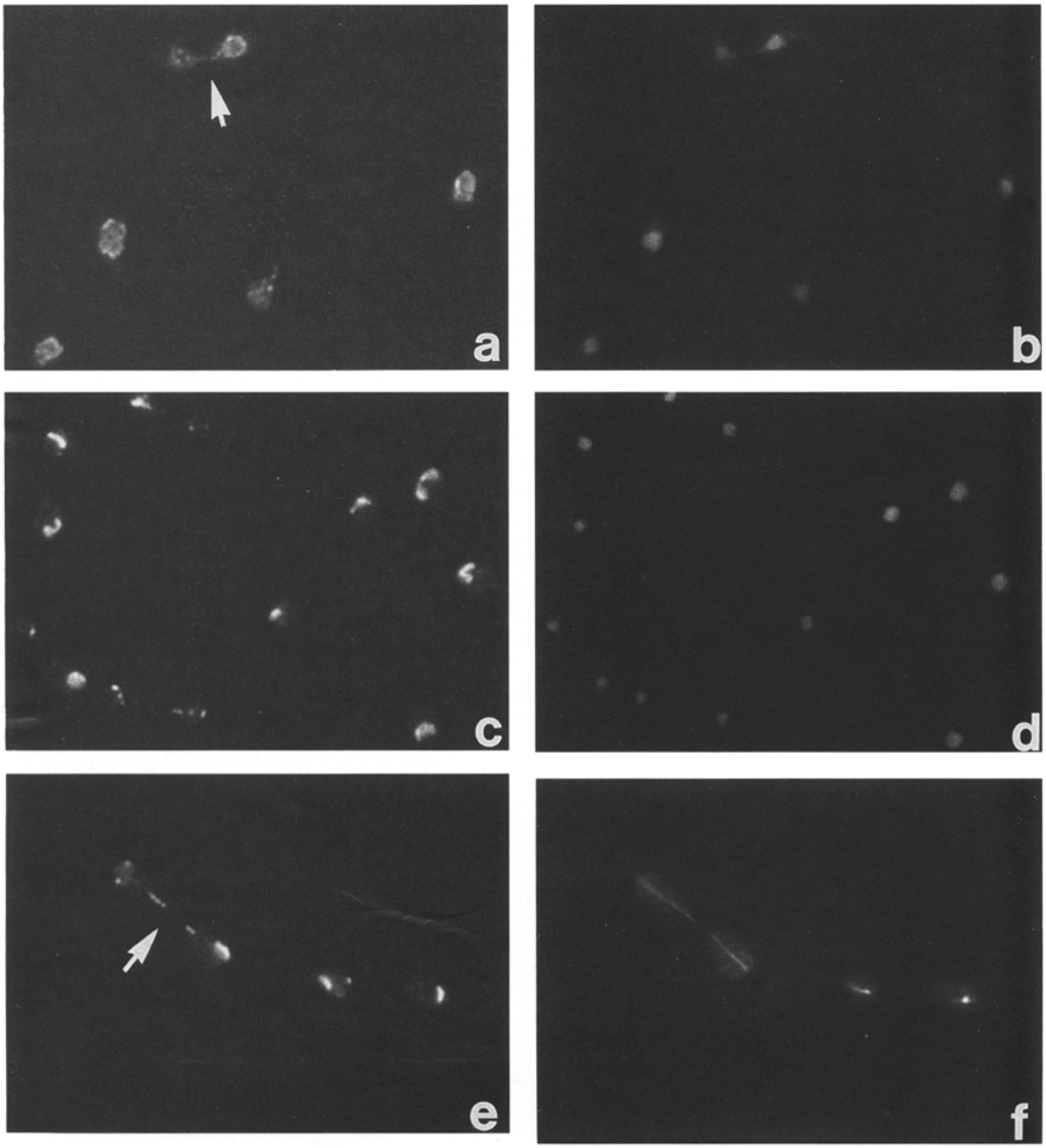

Figure 5. NPC clustering and segregation of NPC clusters in mitotic *rat2-2* cells. Diploid cells were cultured at room temperature, fixed and processed for indirect immunofluorescence microscopy with anti-nuclear pore complex antibody RL1 (*a*, *c*, and *e*) or anti-tubulin (*f*). (*b* and *d*) Corresponding Hoechst 33258 stain for DNA. (*a* and *b*) Wild-type cells. (FY23x86); (*c* and *d*) *rat2-1*/*rat2-1* cells (DAt4xt4); (*e* and *f*) *rat2-2*/*rat2-2* cells (DAt2xt2). The arrowheads indicate mitotic wild-type or *rat2-2*/*rat2-2* cells. Bar, 5 μm.

the *RAT2* open reading frame except for the first 86 and last 60 amino acids were replaced with the *HIS3* gene from pRS403 (Fig. 3 *B*). One copy of the *RAT2* gene in a wild-type diploid strain was disrupted, the strain was transformed with pCH3 containing the wild-type *RAT2* gene and the *URA3* gene, and the diploids were sporulated. From each tetrad, four haploid progeny were observed, two Ura^+ and two Ura^-, indicating that the *RAT2* gene was not required for growth at 23°C, but was required for growth at 37°C. $Poly(A)^+$ RNA accumulated in the nuclei of cells carrying the *rat2Δ* allele following a shift to 37°C (Fig. 1 *M*). Interestingly, the percentage of *rat2Δ* cells showing nuclear accumulation of $poly(A)^+$ RNA at 23°C was consistently lower than that observed in the *rat2-1* strain (5–10% for the *rat2Δ* allele as compared with approximately 15–20% for the *rat2-1* allele). In contrast, while only ~80% of *rat2-1* cells showed nuclear accumulation of $poly(A)^+$ RNA following a 4-h shift to 37°C, the percentage in the *rat2Δ* strain approached 100%.

Immunolocalization of Rat2p

The *RAT2* gene was "tagged" with an epitope-coding sequence to determine the subcellular location of the encoded protein. Three copies of the *myc* epitope recognized by monoclonal antibody 9E10 were inserted into an allele of the *RAT2* gene which had been altered by site-directed mutagenesis to permit introduction of an epitope tag at very near the COOH terminus, between amino acids 1028 and 1029 (out of 1,037). The epitope-tagged *RAT2* construct was able to complement the temperature sensitivity and nuclear $poly(A)^+$ RNA accumulation defects of cells carrying either the *rat2-1* mutation or a disruption of *RAT2*. By indirect immunofluorescence, the epitope-tagged protein was found to be located at the nuclear rim (Fig. 4 *A*). The punctate pattern observed is characteristic of NPC proteins and proteins that associate with nucleoporins. In addition, the fluorescence pattern observed with the anti-*myc* epitope antibody co-localized with that found for monoclonal antibody RL1 (Fig. 4 *B*). The punctate staining pattern and the colocalization of Rat2pmyc and RL1-reactive antigens indicate that Rat2p is a nucleoporin. Therefore, we refer to this protein as Rat2p/Nup120p.

Nuclear Pore Complexes Are Clustered in Yeast Strains Containing Mutant Alleles of the RAT2 Gene and Remain Clustered in Nuclei Isolated from Mutant Cells

The NPC plays a critical role in nucleocytoplasmic transport. Since it contains as many as 100 different polypeptides, we expected that some mutants identified in our screen would have defects in the structure, function, or assembly of NPCs. Therefore, we performed a series of immunofluorescence experiments on yeast strains bearing mutant alleles of *rat2* using antibody RL1, which reacts with nuclear pore complex components in mammalian, amphibian, and yeast cells (Snow et al., 1987; Featherstone et al., 1988; Copeland and Snyder, 1993).

For these experiments we used diploid cells homozygous for the *rat2-1* or *rat2-2* mutations. Immunofluorescence micrographs of wild-type yeast and strains homozygous for the *rat2-1* or *rat2-2* alleles are shown in Fig. 5. In wild-type yeast (Fig. 5 *A*), antibody RL1 stained the nuclear periphery in a discontinuous or punctate manner, a pattern indicative of nuclear pore complex staining. This nuclear rim-staining completely surrounded the DAPI-stained region of the nucleus (Fig. 5 *B*). When *rat2-1* and *rat2-2* cells were stained with antibody RL1, a very different pattern was seen. Instead of a punctate pattern around the nuclear rim, the RL1 antigens were clustered in an area adjacent to rather than surrounding the nuclear DNA (Fig. 5 *C*). In cells carrying the *rat2-1* allele the patch was usually one discrete entity and was often curved or cup-shaped. Little cytoplasmic staining was seen. In cells carrying the *rat2-2* allele (data not shown), the RL1 antigens were more often grouped into two or three smaller patches For both *rat2* mutant strains, all of the cells in the population exhibited the clustering phenotype. Fig. 5 *E* shows the RL1 staining pattern in a *rat2-2* cell in the midst of karyokinesis. It can be seen that both daughter nuclei have received some of the clustered NPCs. The location of the mitotic spindle is shown in Fig. 5 *F*, where an anti-tubulin antibody was used. Clustering of NPC antigens was not altered following a shift to the nonpermissive temperature for up to 4 h (data not shown). We also examined the segregation pattern for NPC clustering when the original strain containing the *rat2-1* allele was backcrossed. The NPC clustering co-segregated with the inability to grow at 37°C and the nuclear accumulation of $poly(A)^+$ RNA following a shift to 37°C. This indicates that NPC clustering is another phenotype associated with mutation of *RAT2*. The NPC clustering observed in strains carrying the *rat2Δ* allele was indistinguishable from that observed in the *rat2-1* strain (data not shown).

Unlike the clustering of NPCs in *rat2* cells, which was observed at permissive as well as restrictive temperatures, accumulation of $poly(A)^+$ in the nucleus was temperature conditional. Nuclear RNA accumulation occurred in nearly all cells at the elevated temperature, but only in a small subpopulation at permissive temperature. We investigated whether the difference in temperature induction of the two phenotypes resulted from a lower threshold temperature for pore complex antigen mislocalization than for $poly(A)^+$ RNA accumulation. To examine this possibility, we performed similar immunofluorescence analyses on

Figure 6. Electron microscopy indicates that nuclear pore complexes are clustered in *rat2* mutant cells. Diploid cells were cultured at room temperature and then shifted to 37°C for 3.5 h prior to fixation and processing for electron microscopy. Nuclear pore complexes, recognized as dark bars at interruptions in the nuclear envelope are distributed around the nuclear envelope in wild-type and rat1-1/rat1-1cells (*small arrowheads*). In *rat2-1/rat2-1* cells (*a* and *b*) the nuclear pore complexes are located in large groups. In some cases the pore complexes are sectioned en face and appear as rings with granules in the center. Spindle pole bodies are visible in *a* and *b* (*b*, *large arrowhead*). The *rat2-1/rat2-1* cell in *b*, is in late mitosis, as indicated by the elongated nuclear envelope and the visible mitotic spindle, which pass out of the plane of section. (*a* and *b*) *rat2-1/rat2-1* cells (DAt4xt4). (*c*) A wild-type diploid cell (FY23x86). (*d*) A rat1-1/rat1-1 cell (DAt1xt1). Bars, 0.5 μm.

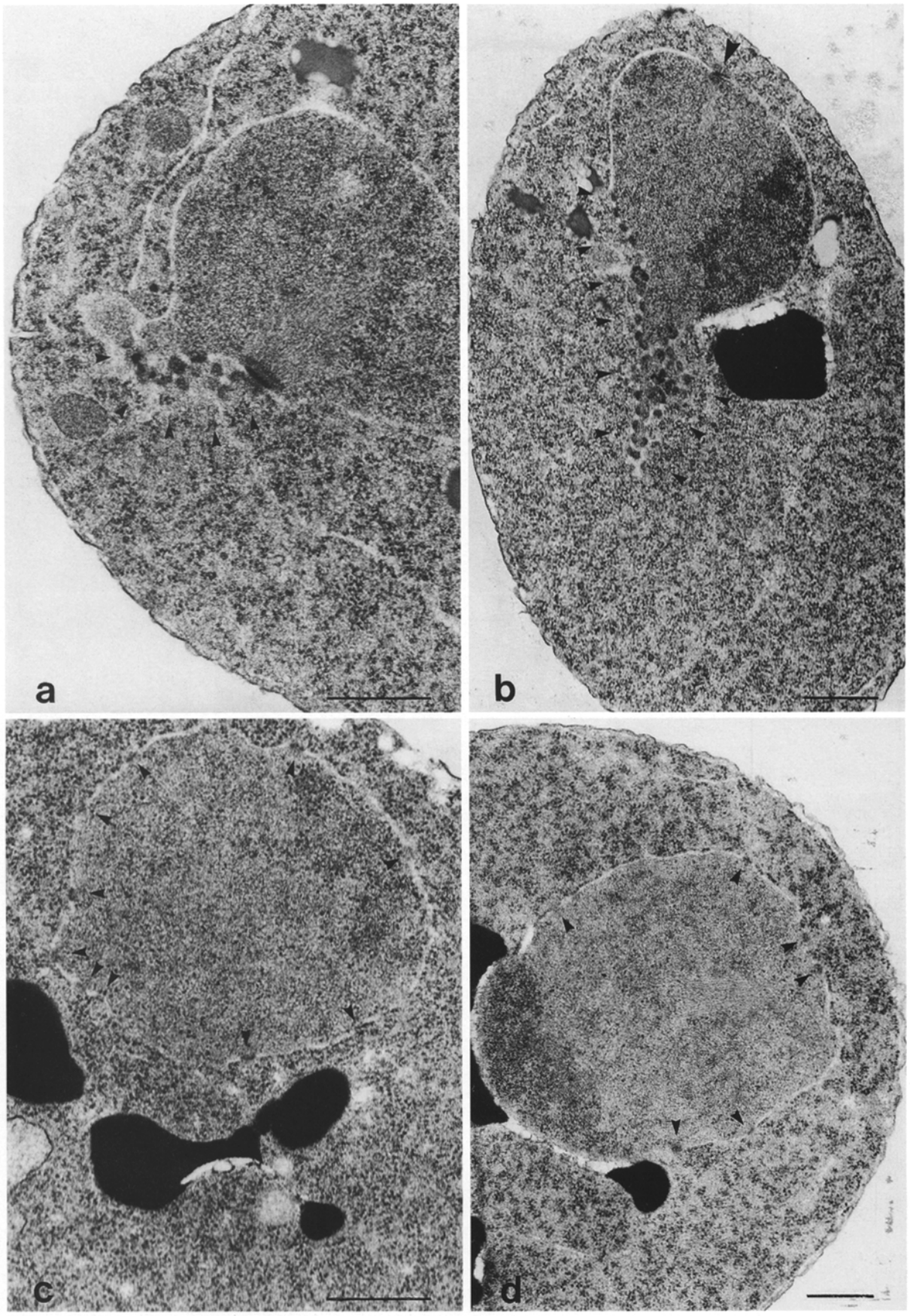
a
b
c
d

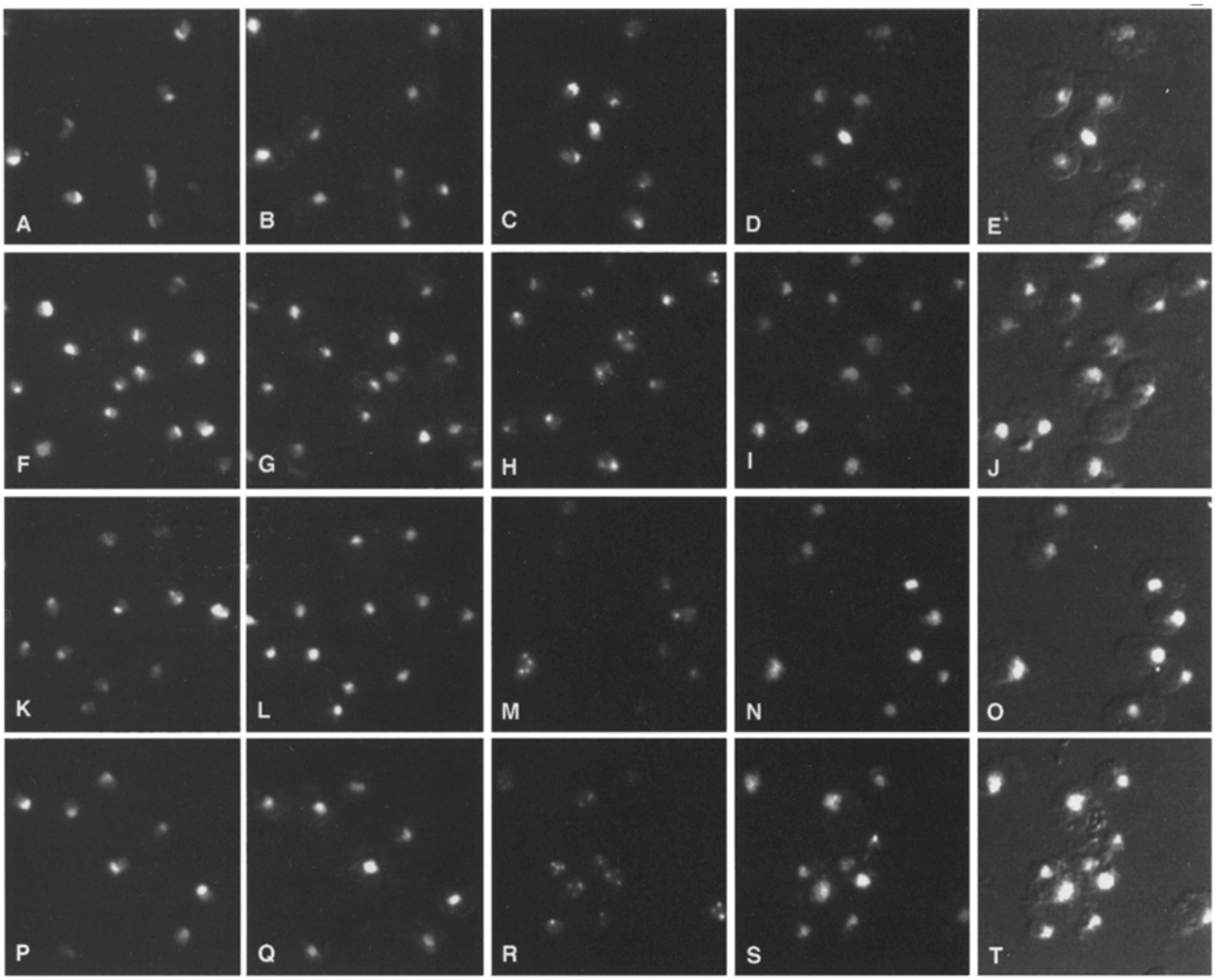

Figure 7. *rat2-1* mutant cells and *rat2Δ* null cells show nucleolar fragmentation when shifted to 37°C. Wild-type (FY23) (*A–E*), *rat2-1* (CCY282) (*F–J*), *rat2Δ* (CHY104) (*K–O*), and *rat7-1* cells (LGY103) (*P–T*) were grown to early log phase in YPD at 23°C. Aliquots either held at 23°C (*A*, *B*, *F*, *G*, *K*, *L*, *P*, and *Q*) or shifted to 37°C for 4 h (*C*, *D*, *E*, *H*, *I*, *J*, *M*, *N*, *O*, *R*, *S*, and *T*) were fixed and analyzed by IF microscopy using monoclonal antibody 2.3B which recognizes the yeast nucleolus, and an FITC-conjugated secondary antibody. (*A*) WT, 23°C, FITC; (*B*) the same field of cells as in *A*, stained with DAPI; (*C*) WT, 37°C, FITC; (*D*) the same field of cells as in *C*, stained with DAPI; (*E*) the same field of cells as in *C*, stained with DAPI and simultaneously viewed by low illumination DIC microscopy; (*F*) *rat2-1*, 23°C, FITC; (*G*) the same field of cells as in *F*, stained with DAPI; (*H*) *rat2-1*, 37°C, FITC; (*I*) the same field of cells as in *H*, stained with DAPI; (*J*) the same field of cells as in *H*, stained with DAPI and simultaneously viewed by low illumination DIC microscopy; (*K*) *rat2Δ*, 23°C, FITC; (*L*) the same field of cells as in *K*, stained with DAPI; (*M*) *rat2Δ*, 37°C, FITC; (*N*) the same field of cells as in *M*, stained with DAPI; (*O*) the same field of cells as in *M*, stained with DAPI and simultaneously viewed by low illumination DIC microscopy; (*P*) *rat7-1*, 23°C, FITC; (*Q*) the same field of cells as in *P*, stained with DAPI; (*R*) *rat7-1*, 37°C, FITC; (*S*) the same field of cells as in R, stained with DAPI; (*T*) the same field of cells as in R, stained with DAPI and simultaneously viewed by low illumination DIC microscopy.

cells cultured at 15°C. Clustering of the pore complex antigens was observed in *rat2-1* and *rat2-2* strains cultured continuously at 15°C. Thus, the *rat2-1* and *rat2-2* mutations caused conditional accumulation of poly(A)$^+$ RNA in the nucleus at nonpermissive temperature (37°C) and constitutive mislocalization of nuclear pore complex antigens at all temperatures tested.

The position of NPCs in wild-type and mutant cells was also examined by electron microscopy. Fig. 6 shows the results of an experiment using diploid cells shifted to 37°C for 3.5 h. For wild-type cells and cells homozygous for the rat1-1 mutation, NPCs were distributed around the nuclear envelope (Fig.6, *C* and *D*) although occasional local concentrations were observed, as has been previously reported (Severs et al., 1976). In contrast, in cells homozygous for the *rat2-1* mutation, NPCs were always observed in one discrete area of the nuclear envelope, frequently in a protuberance, and the rest of the nuclear envelope profile appeared barren of NPCs (Fig. 6, *A* and *B*). When pore complexes of *rat2-1*/*rat2-1* cells were sectioned tangentially, the characteristic structure of a ring and central granule could be seen (Fig. 6, *A* and *B*). Similar NPC clus-

ters were also observed in diploid cells homozygous for the *rat2-2* mutation (data not shown). No gross differences were observed in the morphology of the nucleoplasm or the nucleolus in cells carrying mutant alleles of rat2 as compared to wild-type. The darker, nucleolar region can be observed at the lower right of the nucleus in Fig. 6 *B*, at the upper right in Fig. 6 *C* and at the lower left in Fig. 6 *D*.

Fig. 6 *B* shows a mitotic cell, with part of the spindle pole body and elongated mitotic spindle included in the plane of section. In this cell, a cluster of NPCs was located in the constricted area of the elongated nuclear envelope, possibly migrating between mother and daughter cells. The results from electron microscopy extend the immunofluorescence observations and demonstrate clearly that NPCs were clustered, often in a protuberance of the nuclear envelope. A close association between the spindle pole body and NPC clusters was often seen when the thin section included both the spindle pole body and NPCs. Thus NPCs apparently underwent assembly and insertion into the nuclear membrane in cells carrying the *rat2-1* or *rat2-2* alleles, but failed to become distributed around the nuclear periphery. At this low level of resolution the NPCs appeared to have normal morphology.

To begin to address the mechanism by which NPC clusters were generated, we tested whether the clusters were maintained in nuclei isolated from *rat2* mutant cells. It seemed possible that aberrant connections between nuclear pore complexes and cytoskeletal elements might play a role in the clustering phenotype, and that if these putative connections were broken, pore complexes might be free to redistribute around the nucleus. Subcellular fractions enriched in nuclei were prepared from *rat2-1/rat2-1* cells and from isogenic wild-type cells. We examined in parallel nuclei isolated from *rat3-1/rat3-1* cells. Nuclei were fixed directly and processed for indirect immunofluorescence with antibody RL1. Alternatively, nuclei were incubated at 23° or 30°C for 4–6 h before fixation to allow potential diffusion of NPCs within the nuclear envelope. In this case, clustering of NPCs was maintained in nuclei isolated from *rat2-1/rat2-1* and *rat3-1/rat3-1* cells (data not shown). Thus, the pore complex clusters observed in *rat2* and *rat3* cells do not appear able to redistribute freely around the nuclear envelope when nuclei are separated from cytoplasmic components.

Effect of Mutations of RAT2/NUP120 on Nucleolar Structure and Function

Fragmentation of the nucleolus has been reported for some yeast strains which accumulate poly(A)$^+$ RNA in their nuclei (Kadowaki et al., 1994). To determine whether strains carrying either the *rat2-1* or *rat2Δ* alleles showed a similar nucleolar fragmentation, we performed indirect immunofluorescence using antibodies to two nucleolar proteins, Nop1p (monoclonal antibody A66) and Nsr1p (monoclonal antibody 2.3B). Identical results were obtained with each antibody. The results using antibody 2.3B are shown in Fig. 7. In wild-type cells incubated at 23°C, a brightly staining crescent-shaped pattern was seen in many cells as well as a less brightly staining nucleoplasm. This crescent shaped region is the nucleolus, and the additional staining probably reflects the presence of some nucleolar protein in the nucleoplasm. A dramatic fragmentation of the nucleolus was seen in the *rat7-1/nup159-1* strain shifted to 37°C for 4 h (Fig. 7 *R*); few if any cells had a crescent-shaped staining pattern while most showed from two to six bright spots of fluorescence. Fragmentation could be detected in some cells as soon as 20 min after shifting *rat7-1* cells to 37°C (Gorsch, L. C., and C. N. Cole, unpublished results). Cells carrying mutant alleles of *RAT2* showed a phenotype that was not completely wild-type but was considerably less abnormal than that seen in the *rat7-1/nup159-1* strain (compare Figs. 7, *H* and *M* with *R*). At 37°C, we saw a higher level of staining for nucleolar antigen in the nucleoplasm of *rat2-1* and *rat2Δ* cells than in wild-type cells. While one to four bright fluorescent spots were seen in some mutant nuclei (Fig. 7, *H* and *M*), other nuclei appeared very similar to those of wild-type cells.

To examine whether nucleolar function was affected by mutation of *RAT2*, we analyzed the incorporation of [^{3}H]uridine into ribosomal RNA. 2.5 h after a shift to 37°C, cells carrying the *rat2-1* mutation incorporated approximately 50% as much [^{3}H]uridine into TCA-precipitable material as did wild-type cells while cells carrying the *rat7-1/nup159-1* mutation incorporated less than 10% as much [^{3}H]uridine as wild-type cells after a 30-min shift to 37°C (data not shown). Labeled RNA was analyzed by electrophoresis and fluorography (Fig. 8). The patterns of incorporation were essentially the same for wild-type and *rat2-1* mutant cells; mature 18S and 25S rRNA and precur-

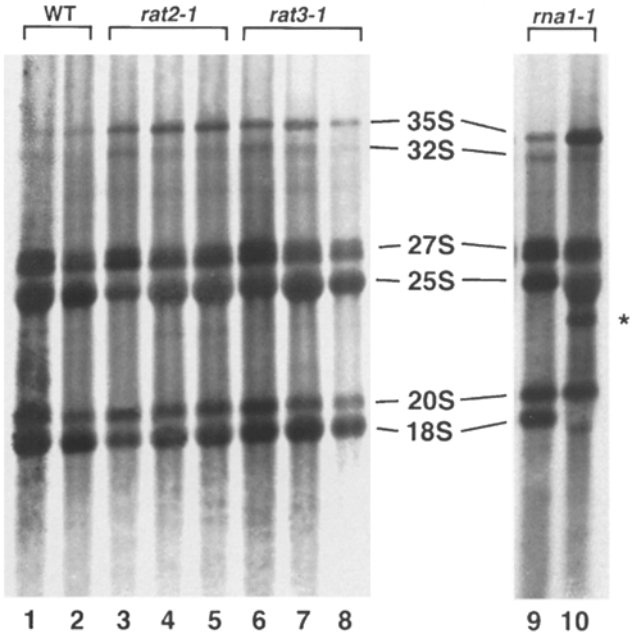

Figure 8. rRNA processing and export occur normally in *rat2-1* and *rat3-1* cells. [^{3}H]Uridine-labeled RNA was isolated from several strains and analyzed by electrophoresis in a 1.2% agarose–formaldehyde gel. (Lane *1*) WT (FY86) grown at 23°C; (lane *2*) WT shifted to 37°C for 3.5 h; (lane *3*) *rat2-1* grown at 23°C; (lane *4*) *rat* 2-1 shifted to 37°C for 2.5 h (lane *5*) *rat2-1* shifted to 37°C for 3.5 h; (lane *6*) *rat3-1* grown at 23°C; (lane *7*) *rat3-1* shifted to 37°C for 2.5 h; (lane *8*) *rat3-1* shifted to 37°C for 3.5 h.; (lane *9*) *rna1-1* grown at 23°C; (lane *10*) *rna1-1* shifted to 37°C for 40 min (*) indicates position of a 23 S intermediate product produced during rRNA processing and accumulating in the *rna1-1* mutant strain.

sor 20S and 27S rRNAs were readily seen. Thus, synthesis and processing of rRNA appeared normal. As a control, we examined a strain which is known to have defects in rRNA processing and which contained the *rna1-1* allele (Traglia et al., 1989). While the pattern seen at 23°C in the *rna1-1* strain was indistinguishable from wild-type (compare lanes *1* and *9*), precursor 35S and 32S pre-rRNAs accumulated in the *rna1-1* strain following a shift to 37°C (lane *10*), aberrantly processed species accumulated (see *asterisk* at right of lane *10*), and little 18S rRNA accumulated. We conclude that mutation of *RAT2/NUP120* had a minimal affect on the synthesis and processing of ribosomal RNAs even though some morphological alterations to the nucleolus were detected.

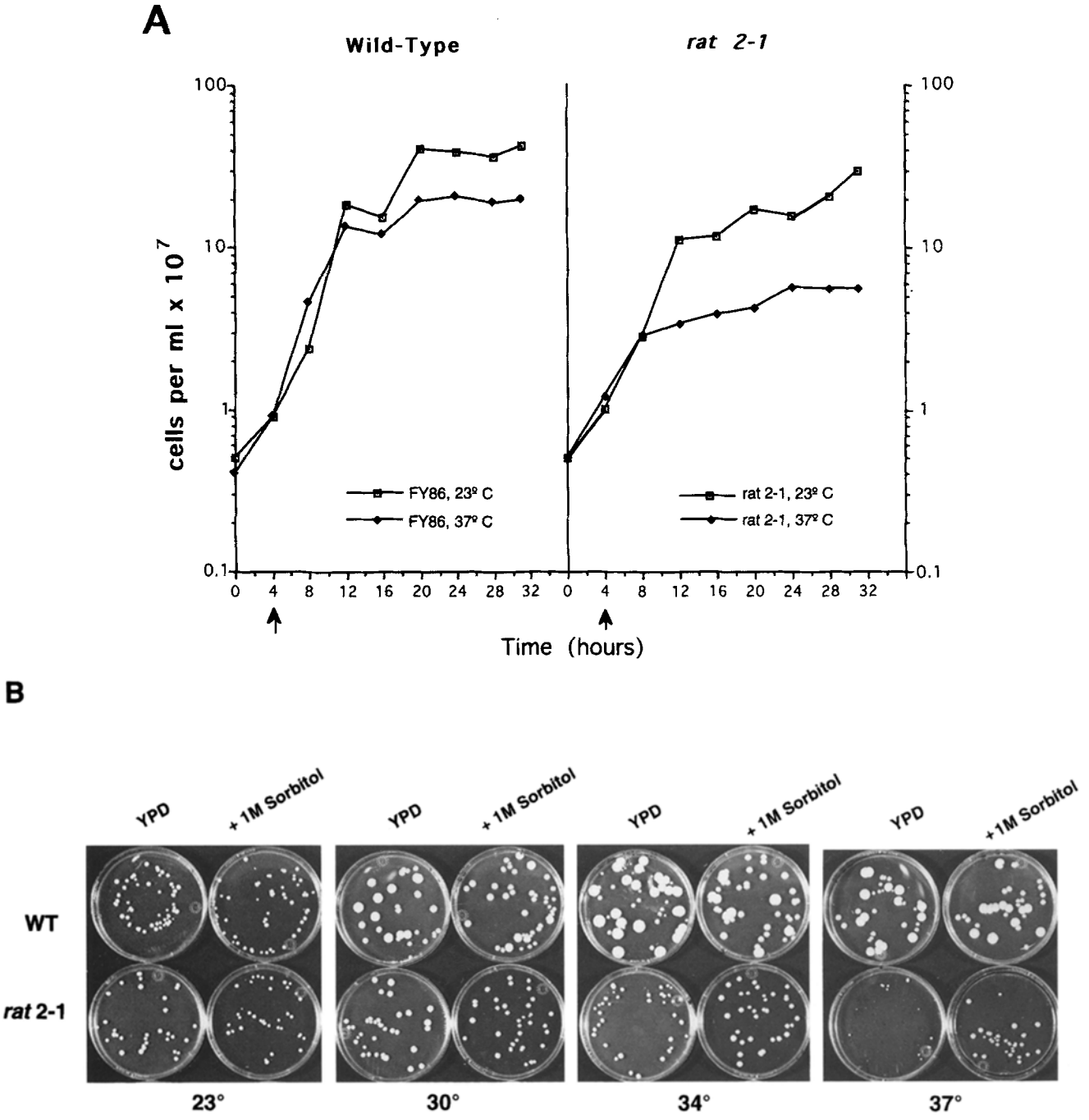

Figure 9. Growth properties of yeast cells carrying the *rat2-1* mutation. (*A*) Growth curves of wild-type (FY23) and *rat2-1* cells (CCY282). Cells were grown at 23°C to early log phase. After 4 more hours growth at 23°C, aliquots of each strain were shifted to 37°C and growth curves were made by counting cells every 4 h. (*B*) Growth characteristics of wild-type (FY23) and *rat2-1* (CCY282) cells grown on plates containing either YPD or YPD supplemented with 1.0 M sorbitol. Overnight cultures of wild-type (FY23) and *rat2-1* cells (CCY282) cells were diluted and grown on YPD or YPD/1.0 M sorbitol plates at 23°, 30°, 34°, or 37°C. The *rat2-1* cells form colonies at 23°C but cannot do so 37°C on YPD plates. The addition of 1.0 M sorbitol allowed the *rat2-1* cells to form colonies at 37°C. The plates were photographed after 14 d of growth.

Growth Properties of rat2 Mutant Strains and Suppression of Temperature-sensitive Growth Defects by Sorbitol

A culture of cells carrying the *rat2-1* allele was examined for growth characteristics and the results are shown in Fig. 9 *A*. The wild-type culture (FY86) had a doubling time of approximately 2 h at 23°C. The *rat2-1* strain grew more slowly at this temperature with a doubling time of almost 3.0 h. After the shift to 37°C, the growth rate of the wild-type strain was unaltered but it grew to a lower final density at 37° than at 23°C. After the shift to 37°C, the *rat2-1* mutant strain continued to grow at approximately the same rate at 37°C as it had at 23°C for the next 4 h. Doubling times for the culture increased dramatically beyond this point. The *rat2-1* strain showed a doubling time of approximately 12–15 h during the latter part of the experiment, and reached a final cell density substantially below that obtained under continuous growth at 23°C. A portion of the mutant culture incubated at 37°C was removed after 28 h of incubation and tested for the presence of revertants by plating cells at both 23° and 37°C. No colonies were formed during 7 d of growth on plates incubated at 37°C, indicating that growth of revertants did not contribute to the growth behavior observed in this experiment.

We also examined the growth properties of cells carrying the *rat2-1* mutation on YPD plates incubated at 23°, 30°, 34°, and 37°C (Fig. 9 *B*). Under these conditions, colonies formed by wild-type and mutant cells grown at 23°C were indistinguishable. Mutant colonies formed on plates incubated at 30° and 34°C were considerably smaller than wild-type cells colonies. Very tiny colonies could be seen when plates containing *rat2-1* cells were incubated at 37°C for 14 d. The inclusion of either 1.0 M sorbitol or 0.9 M NaCl in the YPD plates reduced the size of the colonies formed by wild-type cells. These supplements had little effect on mutant colony size for mutant cells incubated at 23°C and caused a slight reduction in colony size following incubation at 30°C. In contrast, these supplements enhanced the size of colonies formed at 34°C. At 37°C, these supplements permitted cells containing the *rat2-1* allele to form colonies. The growth behaviors of the strain carrying a disruption of *RAT2* were the same as those seen with the *rat2-1* strain, in media either with and without 1.0 M sorbitol (data not shown). These results indicate that maintenance of osmotic stability overcame the deleterious effects of the mutations on growth properties.

We wished to determine how the presence of 1.0 M sorbitol affected the various mutant phenotypes seen in *rat2-1* cells. Fig. 10 shows representative micrographs from an experiment where the distribution of poly(A)$^+$ RNA was determined by in situ hybridization (Fig. 10 *B*) and the location and clustering of NPCs was determined by indirect immunofluorescence with an anti-Rat7p/Nup159p antibody (Fig. 10 *A*). Cultures were incubated overnight at 23°C in the presence of sorbitol and were subsequently shifted to 37°C for 4 h in the presence of sorbitol. The data indicate that growth in the presence of sorbitol had no effect on the clustering of NPCs (compare Fig. 10 *A*, panels *D* and *E*). The accumulation of poly(A)$^+$ RNA in nuclei of *rat2-1* cells was not completely suppressed by sorbitol, but the nuclear fluorescence was much weaker in the presence of 1.0 M sorbitol (compare Fig. 10 *B*, panels *D* and *E*), suggesting that sorbitol acted to enhance RNA export to a degree sufficient to permit continued growth, but that the suppression of the nuclear accumulation of poly(A)$^+$ RNA was not complete. Interestingly, a modest accumulation of poly(A)$^+$ RNA was seen in the nuclei of some wild-type cells cultured in the presence of 1.0 M sorbitol and incubated at 37°C (Fig. 10 *B*, panel *B*).

Synthetic Lethality

Two mutations are said to be synthetically lethal if yeast strains carrying either mutation can grow but strains carrying both are unable to do so (Bender and Pringle, 1991; Costigan et al., 1992). Synthetic lethality has been used to provide insight into whether two gene products interact, are part of the same macromolecular complex, or are redundant. Synthetic lethality has been observed between mutant alleles of several nucleoporins (for review see Doye and Hurt, 1995) and has also been observed between nucleoporins and proteins that interact with nucleoporins but are themselves not components of the NPC (Belanger et al., 1994). Synthetic lethality analyses are performed by mating strains carrying mutations of interest, introducing into the heterozygous diploid a *CEN URA3* plasmid containing the wild-type allele of one of the genes being tested, sporulating, dissecting tetrads, and determining whether those resulting haploids carrying mutant alleles of both genes require the presence of a wild-type allele of one of the genes for growth. Strains heterozygous for both *rat2-1* and *rat3-1/nup133-1* or for both *rat2-1* and *rat7-1/nup159-1* were sporulated, tetrads were dissected, and progeny haploid strains were analyzed. All of the 24-spore tetrads obtained from the diploid heterozygous for *rat2-1* and *rat3-1/nup133-1* yielded one or more haploid strains unable to grow on 5-FOA (see Materials and Methods). From the diploids heterozygous for *rat2-1* and *rat7-1*, only five tetrads yielding four viable haploid strains were obtained. For each, one of the four strains was unable to grow on 5-FOA. Since *RAT2/NUP120* is not linked to either *RAT7/NUP159* or *RAT3/NUP133*, this indicates that *rat2-1* is synthetically lethal with both *rat7-1/nup159-1* and *rat3-1/nup133-1*.

Discussion

In this paper, we have described the cloning and characterization of the *RAT2/NUP120* gene of *S. cerevisiae*, which encodes a 120.4-kD protein. We refer to this protein as Rat2p/Nup120p. We believe that this protein is a nucleoporin based on the following findings: (*a*) epitope-tagged, Rat2p was found to be located at the nuclear rim in a punctate pattern diagnostic of NPC proteins; (*b*) the staining pattern for $Rat2p_{myc}$ was identical to that seen with the RL1 monoclonal antibody, which is known to recognize yeast nucleoporins; (*c*) NPCs were clustered in the nuclear envelope of cells carrying mutant alleles of *RAT2*. This phenotype has been observed in strains carrying mutant alleles of several nucleoporins and has not been associated with mutations of other classes of genes. (*d*) Synthetic lethality was observed between the *rat2-1* allele and mu-

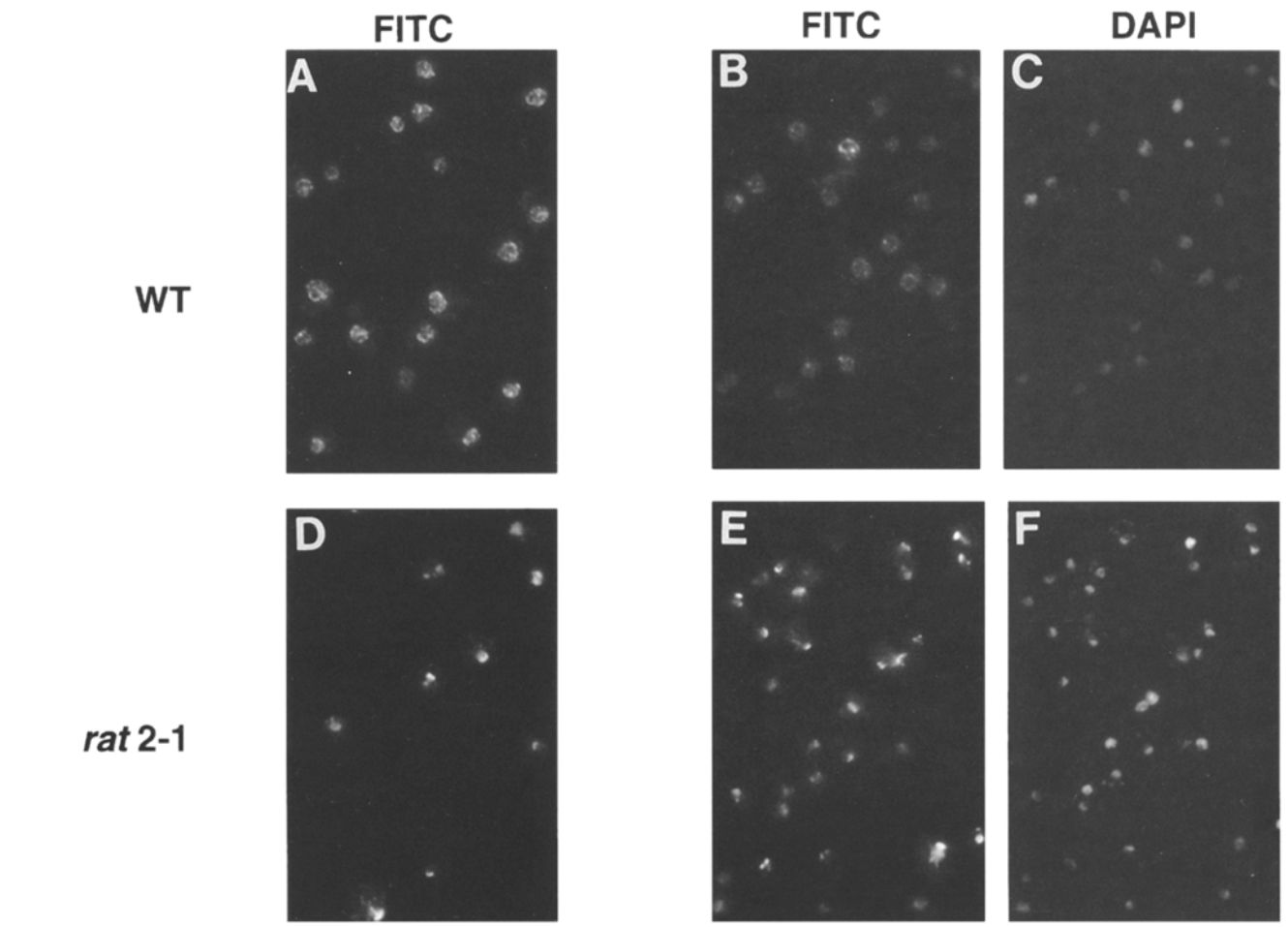

Figure 10. Effect of 1.0 M sorbitol on NPC clustering and poly(A)$^+$ RNA distribution phenotypes in *rat2-1* mutant cells. (*A*) IF of wild-type (FY23) (panels *A–C*) and *rat2-1* cells (CCY282) (panels *D–F*) using an anti-Rat7p/Nup159p antibody and an FITC-conjugated secondary antibody. Cultures were incubated overnight at 23°C in either YPD or YPD + 1.0 M sorbitol and were shifted to 37°C for 4 h. (Panel *A*) WT grown on YPD and shifted to 37°C, FITC; (*B*) WT grown on YPD + 1.0 M sorbitol and shifted to 37°C, FITC; (*C*) the same field of cells as in panel *B*, stained with DAPI; (*D*) *rat2-1* cells grown on YPD and shifted to 37°C, FITC; (*E*) *rat2-1* cells grown on YPD + 1.0 M sorbitol and shifted to 37°C, FITC; (*F*) the same field of cells as in panel *E*, stained with DAPI. *rat2-1* cells grown on YPD + 1.0 M sorbitol at 37°C still display clustering of NPCs (compare panels *A* and *B*). (*B*) Localization of poly(A)$^+$ RNA, visualized with a FITC-conjugated anti-digoxigenin antibody. Cultures were prepared as in *A*. (Panel *A*) WT cells grown on YPD and shifted to 37°C, FITC; (*B*) WT cells grown on YPD + 1.0 M sorbitol and shifted to 37°C, FITC; (*C*) the same field of cells as in panel *B*, stained with DAPI; (*D*) *rat2-1* cells grown on YPD and shifted to 37°C, FITC; (*E*) *rat2-1* cells grown on YPD + 1.0 M sorbitol and shifted to 37°C, FITC; (*F*) the same field of cells as in panel *E*, stained with DAPI. The accumulation of poly(A)$^+$ RNA in the nuclei of the *rat2-1* cells grown on YPD + 1.0 M sorbitol at 37°C was not completely suppressed, but the nuclear fluorescence was much weaker (compare panels *D* and *E*).

tant alleles of *RAT3/NUP133* and *RAT7/NUP159*. Rat2p/Nup120p is the fourth yeast nucleoporin identified that lacks the repeat motifs found in the majority of nucleoporins described to date. Nic96p, Rat3p/Nup133p, and Nup82p are the other three yeast nucleoporins lacking repeats.

Nucleocytoplasmic Export of Poly(A)$^+$ RNA

Poly(A)$^+$ RNA accumulated in the nuclei of *rat2-1* and *rat2Δ* mutant cells after a shift to 37°C. A low percentage of cells showed nuclear poly(A)$^+$ RNA accumulation at 23° or 15°C while most cells showed this phenotype within 4 h of a shift to 37°C. The RNA accumulation phenotype of these mutant strains was much less dramatic than we saw in strains with mutant alleles of *RAT7/NUP159* (Gorsch et al., 1995). In the latter case, 100% of the cells showed bright nuclear fluorescence (reflecting accumulation of poly[A]$^+$ RNA) within 30 min of a shift to 37°C.

Several explanations are possible for the gradual and slow appearance of the RNA export defect in *rat2-1* and *rat2Δ* cells. Repeat-containing nucleoporins may be located along the entire axis of the NPC, from the nuclear basket to the cytoplasmic filaments. This would enable them to interact with substrate (either protein or RNP)

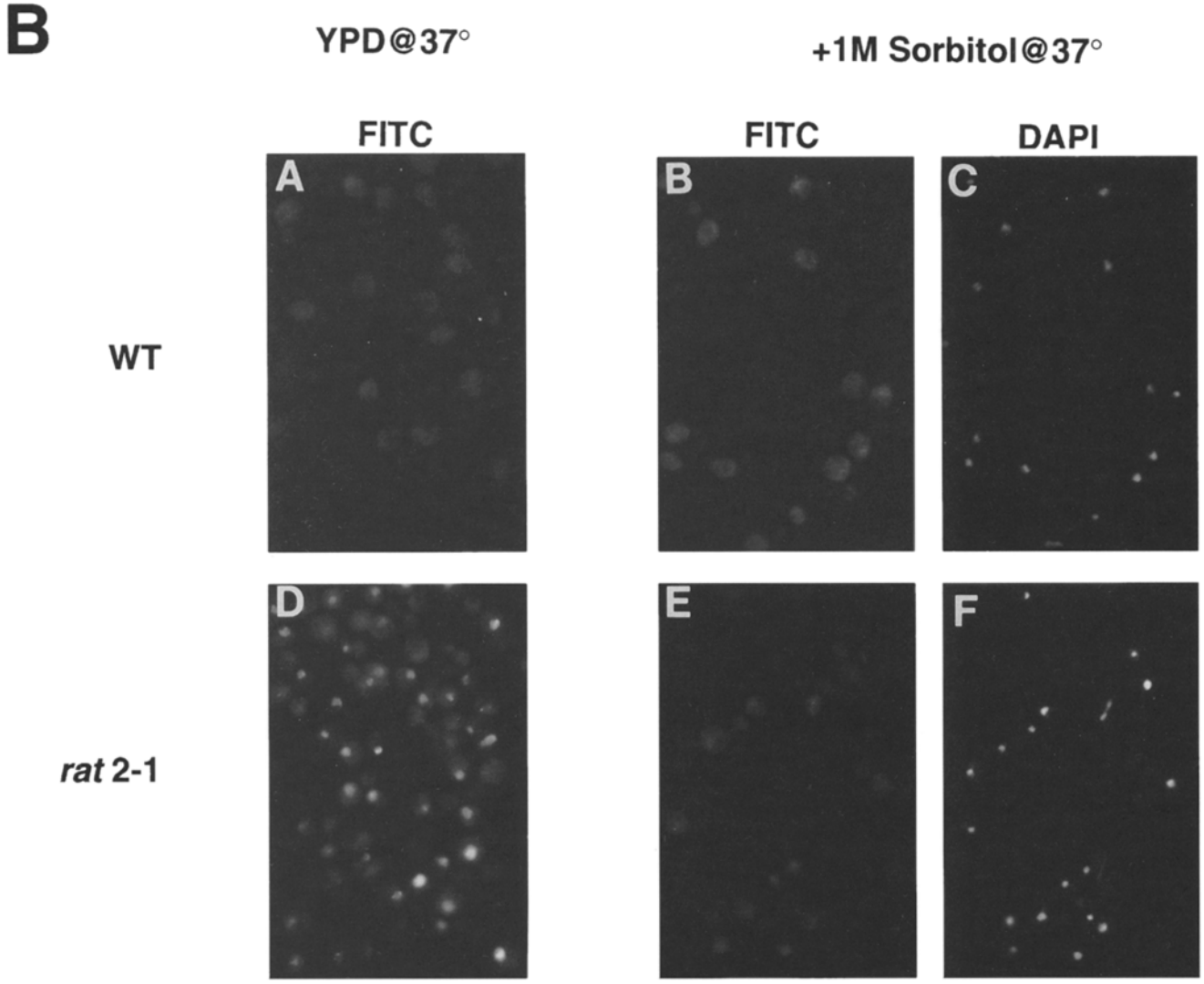

which could be passed along from one repeat–containing nucleoporin to another (Radu et al., 1995). Nucleoporins lacking repeats, such as Rat2p/Nup120p, could play a role in anchoring repeat-containing nucleoporins within the overall NPC framework. Complexes can be isolated that contain both repeat-containing and nonrepeat-containing nucleoporins (Grandi et al., 1993, 1995*a*,*b*). If such complexes were normally anchored by more than one NPC protein, loss of one of these (by disruption of the gene encoding it) might permit retention of function at 23°C, but shifting cells to 37°C could cause the complex to dissociate from NPC. By this model, Rat2p/Nup120p and some other NPC protein could work together to anchor such a complex in the pore framework. A related possibility is that the putative Rat2p/Nup120p-containing complex is absent from NPCs at all temperatures but that the mutant NPCs retain an ability to export RNA at 15° and 23°C. Such altered pores might be thermosensitive and could undergo greater loss of function following a shift of mutant cells to 37°C. Whatever changes in pore structure and function occur following a temperature shift, they do not appear to cause overall failure of all NPC functions, since no defect in import of nuclear proteins was observed in *rat2-1* cells.

Alterations to Nucleolar Structure in Mutant Strains

Modest alterations in nucleolar structure were seen by indirect immunofluorescence when *rat2*/nup120 mutant cells were shifted to 37°C. However, the continued incorporation of [^{3}H]uridine into rRNA and its normal processing into 18S and 25S rRNA suggests that whatever alterations occurred to nucleolar structure, nucleolar functions were not compromised. Since the final processing of 20S to 18S rRNA is thought to occur in the cytoplasm (Udem and Warner, 1973), export of ribosomal subunits must still be occurring 3.5 h following a shift of *rat2-1* cells to 37°C since labeled 18S rRNA was produced and the ratio of 20S to 18S rRNA was very similar in wild-type and mutant strains shifted to 37°C. This is in contrast to the dramatic disruption of the nucleolus following shift to 37°C of strains carrying the *rat7-1* allele; in that strain, synthesis and processing of rRNA ceased very rapidly following the shift.

How mutations in NPC proteins might affect nucleolar structure and function is uncertain. One possibility is that there are direct connections between NPCs and nucleolar components. The yeast nucleolus lies closely apposed to the nuclear envelope (see Fig. 6), and this arrangement

may facilitate efficient export of ribosomal subunits. Perhaps these interactions are sensitive to disruption in strains lacking specific nucleoporins or containing altered NPC proteins. Alternatively, nucleolar alteration or fragmentation could reflect an indirect effect caused by a block to the export of ribosomal subunits. Perhaps accumulation of rRNA within the nucleus signals the nucleolus to cease production of additional ribosomal subunits. If the processing of 20S to 18S rRNA can be taken as evidence for rRNA export, rRNA export continued after a shift of *rat2* mutant strains to 37°C. Although incorporation of [^{3}H]uridine into rRNA was reduced approximately 50%, processing appeared normal (Fig. 8). Thus, the slightly altered nucleoli in *rat2* mutant strains appeared to function quite well at 37°C. In contrast, fragmentation of the nucleolus occurred rapidly in cells carrying the *rat7-1/nup159-1* allele (within 30 min; our unpublished results); biogenesis of ribosomes also ceased very soon following a shift of *rat7-1/nup159-1* cells to 37°C.

Nuclear Pore Complex Clustering

We have described clustering of NPCs in yeast strains with mutations of *RAT3/NUP133* (Copeland, C. S., D. C. Amberg, and C. N. Cole. 1991. *J. Cell Biol.* 115:317a; Li et al., 1995) and *RAT7/NUP159* (Gorsch et al., 1995). NPC clustering has also been reported for strains with mutations of *NUP116* (Wente et al., 1992; Wente and Blobel, 1993), and *NUP145* (Fabre et al., 1994; Wente and Blobel, 1994; Dockendorff, T. C., A. L. Goldstein, and C. N. Cole, manuscript in preparation). We have also found NPC clustering in yeast strains carrying a disruption of the *RAT9/NUP85* gene (Goldstein, A. L., and C. N. Cole, manuscript in preparation). In most of these strains, clustering was constitutive, while in strains with the *nup159-1/rat7-1* allele, clustering was reversed following a shift to 37°C and the mutant Rat7p/Nup159p appeared to dissociate from the NPCs following temperature shift. In some of these mutant strains, nuclear envelope defects were also observed, with NPCs clustering together in abnormally structured regions of the nuclear envelope. In other mutant strains (e.g., *rat7-1/nup159-1*), no nuclear envelope abnormalities were observed, and a region of nuclear envelope could be seen surrounding each NPC in a linear cluster. Thus, in different mutant strains, NPC clustering may reflect defects in different aspects of NPC biogenesis and behavior. These mutant strains should be useful for investigating NPC biogenesis and inheritance.

It is not known whether NPCs are assembled at a single site in the nuclear envelope or at many sites. If at a single site, the NPC clustering would reflect a failure to distribute NPCs around the nuclear envelope. If inserted at many sites, the clustering would most likely reflect the aggregation of NPCs containing nucleoporins, perhaps due to exposure of protein domains that are normally hidden in wild-type NPCs but which become exposed in mutant NPCs and can interact with similar domains of other NPCs in mutant strains. Examination of isolated nuclei indicates that, once formed, the NPC clusters do not redistribute in the absence of gross connections to the cytoskeleton. Thus the presence of NPC clusters does not depend on the continuous presence of an intact cytoskeleton. Since clustering of NPCs and other abnormalities of NPC distribution and nuclear envelope morphology have been seen in strains carrying mutant alleles of several nucleoporins, it is unlikely that each of these nucleoporins plays a direct role in the distribution of NPCs. Rather, we favor the idea that the NPC clustering observed reflects a failure to distribute NPCs. Since clusters of NPCs were often seen near to the spindle pole body in *rat2* (for example see Fig. 6 *a*) and *rat3* mutant cells (Copeland, C. S., D. C. Amberg, M. Snyder, and C. N. Cole, unpublished results), we hypothesize that the spindle pole body provides the site for insertion of NPCs into the nuclear envelope. This suggests that synthetic lethality might be found between components of the spindle pole body and some nucleoporins; direct protein–protein interactions between NPC and spindle pole body components would also be expected.

Growth Defects and Their Suppression by High Osmolarity Media

What blocks growth of *rat2* cells at nonpermissive temperature? The experimental results indicate that nuclear pore complex clustering is not sufficient to block growth and slows cell growth and division only slightly for the first several hours following a temperature shift to 37°C. The reduced growth rate at 37°C may be secondary to the RNA export defect and could result from loss of critical cellular functions encoded by genes which produce inabundant and short-lived mRNAs or proteins. The increase in growth rate when cells were grown with osmotic support suggests that an essential function altered by the *rat2* mutations at 37°C may relate to osmotic balance. An increase in extra cellular osmolarity results in a large number of changes in the yeast cell. These include reorganization of the actin cytoskeleton (Chowdhury et al., 1992), induction of an osmosensing signal transduction pathway (Brewster et al., 1993), alterations in gene expression including induction of some of the heat shock genes (Varela et al., 1992), and a large increase in intracellular glycerol level (Edgley and Brown, 1983; Reed et al., 1987). These effects can dramatically alter the expression of mutant phenotypes and this phenomenon has been exploited in the isolation of both osmotic-remedial and osmotic-sensitive mutations (Megnet, 1966; Bassel and Douglas, 1968; Metzenberg, 1968). The mechanisms by which a rise in extracellular osmolarity can affect the expression of mutant phenotypes are poorly understood.

Changes in intracellular glycerol concentrations in response to alterations in osmolarity could alter the properties of the intracellular environment, thereby stabilizing protein–protein interactions within the NPCs. Since high osmotic strength media suppresses the phenotypic defects of strains with a null mutation of *RAT2*, perhaps the large increase in intracellular glycerol which occurs in response to high osmotic strength media stabilizes protein–protein interactions, which may be weaker in NPCs lacking Rat2p. Alternatively, osmo-induced signal transduction pathways described by Gustin and colleagues (Chowdhury et al., 1992; Brewster et al., 1993) could be responsible for the expression of genes whose products reduce the cell's requirement for Rat2p/Nup120p functions. It is also possible that greater osmotic support stabilizes the nuclear enve-

lope or interactions between the nuclear envelope and the NPCs in mutant cells. A similar enhancement of growth defects by high osmolarity media was seen in strains carrying mutant alleles of *RAT7/NUP159*, *RAT3/NUP133*, and *NUP116*, but not in strains with mutant alleles of *RAT9/NUP85* or *RAT10/NUP145* (Heath, C. V., and C. N. Cole, unpublished results).

Identical Phenotypes in rat2 and rat3 Mutant Strains

The phenotypes observed in strains with mutant alleles of *RAT2/NUP120* are strikingly similar to those seen in strains with mutant alleles of *RAT3/NUP133*. In both cases, a small percentage of cells showed nuclear accumulation of poly(A)$^+$ RNA at 23°C and the percentage was much higher following a shift to 37°C. In both cases, accumulation in 100% of the cells was seen with the disruption allele but not with the originally isolated *rat2-1* or *rat3-1* alleles. With both *rat2/nup120* and *rat3/nup133* mutant strains, constitutive clustering of NPCs was observed. No other defects in nuclear structure were seen in either strain except for the modest alteration to nucleolar structure reported here for *rat2-1* cells. We have not yet examined the *rat3-1* strains for nucleolar defects but it showed the same modest decrease in [^{3}H]uridine incorporation and the same normal pattern of 27, 25, 20, and 18 S rRNA species as seen in the *rat2-1* strain (Fig. 8). In both *RAT2/NUP120* and *RAT3/NUP133* mutant strains, growth defects were suppressed by high osmolarity. Finally, the *rat2-1* allele was synthetically lethal with the *rat3-1* allele. While some of these properties are shared with some other strains carrying mutant nucleoporin genes, no other mutant strains share all of the phenotypes shared by *rat2/nup120* and *rat3/nup133* mutant strains.

The *RAT2/NUP120* and *RAT3/NUP133* proteins lack any significant homology with each other or with other known proteins. Rat2p/Nup120p and Rat3p/Nup133p are acidic proteins with pIs of 4.86 and 4.82, respectively. Although no significant alignment of Rat2p/Nup120p with Rat3p/Nup133p was achieved using either the FASTA program or a Pustell matrix analysis, the two have almost identical amino acid compositions. Rat2p contains 41% nonpolar residues, 35.6% polar residues, 12.5% acidic residues, and 10.9% basic residues; for Rat3p/133p, the percentages are 39.9, 35.0, 13.6, and 11.5%, respectively. We do not understand the significance of this similarity nor whether these two proteins interact directly.

In summary, strains carrying mutations of the *RAT2/NUP120* gene show constitutive clustering of nuclear pore complexes that are often seen very close to the spindle pole body. When these cells are shifted to 37°C, we observed a defect in the nucleocytoplasmic export of poly(A)$^+$ RNA and some alterations in the structure of the nucleolus. However, synthesis and normal processing of rRNA continued, suggesting that little or no loss of nucleolar function occurred. Major questions remain concerning the actual functions of Rat2p/Nup120p. Is its primary role in insertion of NPCs or NPC subassemblies into the nuclear envelope? Is it a component of an NPC subassembly which plays a direct role in export of RNA? By what mechanism do mutations within nucleoporins affect nucleolar structure and function? Both genetic and biochemical approaches can be employed to identify proteins with which Rat2p/Nup120p interacts, and this should provide additional insight into its functions.

We thank Larry Gerace for providing antibody RL1, John Aris for providing antibody A66, S. Rasmussen, for providing DNA sequence information for *S. cerevisiae* chromosome XI prior to its publication, Jiyue Zhu and J. Michael Bishop for hybridoma cells, and Joel Rosenbaum and Dan Finley for use of equipment. We thank Beth Jones, Marjorie Brandriss, Anita Hopper, and Fred Winston for providing strains. C. S. Cole thanks Barry Piekos for advice and assistance with electron microscopy and Frank McKeon for providing laboratory space for completion of a portion of this work. We thank Ken Orndorff for assistance with microscopy. We thank Tom Dockendorff and Alan Goldstein for critically reading this manuscript. We are also grateful to the members of the Cole laboratory for interesting discussions and technical advice.

This work was supported by grants from the National Institutes of Health, Public Health Service (GM33998 to C. S. Cole and NIH GM36494 to M. Snyder), by a core grant to the Norris Cotton Cancer Center of Dartmouth Medical School (CA16038) and by a Pew Scholar Award to M. Snyder. C. S. Cole was supported in part by the Department of Radiation Oncology, University of Massachusetts Medical Center, and by a Charles A. King Trust Fellowship from the Medical Foundation.

Received for publication 15 September 1995 and in revised form 13 October 1995.

References

Akey, C. W. 1989. Interactions and structure of the nuclear pore complex revealed by cryo-electron microscopy. *J. Cell Biol.* 109:955–970.

Akey, C. W. 1990. Visualization of transport-related configurations of the nuclear pore transporter. *Biophys. J.* 58:341–355.

Akey, C. W. 1991. Probing the structure and function of the nuclear pore complex. *Semin. Cell Biol.* 2:167–177.

Akey, C. W., and M. Radermacher. 1993. Architecture of the Xenopus nuclear pore complex revealed by three-dimensional cryo-electron microscopy. *J. Cell Biol.* 122:1–19.

Allen, J. L., and M. G. Douglas. 1989. Organization of the nuclear pore complex in *Saccharomyces cerevisiae*. *J. Ultrastcr. Mol. Struct. Res.* 102:95–108.

Amberg, D. A., A. L. Goldstein, and C. N. Cole. 1992. Isolation and characterization of RAT1: an essential gene of *Saccharomyces cerevisiae* required for the efficient nucleocytoplasmic trafficking of mRNA. *Genes & Dev.* 6:1173–1189.

Amberg, D. C., M. Fleischmann, I. Stagljar, C. N. Cole, and M. Aebi. 1993. Nuclear PRP20 protein is required for mRNA export. *EMBO J.* 12:233–241.

Aris, J. P., and G. Blobel. 1988. Identification and characterization of a yeast nucleolar protein that is similar to a rat liver nucleolar protein. *J. Cell Biol.* 107:17–31.

Aris, J. P., and G. Blobel. 1989. Yeast nuclear envelope proteins cross react with an antibody against mammalian pore complex proteins. *J. Cell Biol.* 108:2059–2067.

Bassel, J., and H. C. Douglas. 1968. Osmotic remedial response in a galactose negative mutant of *Saccharomyces cerevisiae*. *J. Bacteriol.* 95:1103–1110.

Belanger, K. D., M. A. Kenna, S. Wie, and L. I. Davis. 1994. Genetic and physical interactions between Srp1p and nuclear pore complex proteins Nup1p and Nup2p. *J. Cell Biol.* 126:619–630.

Bender, A., and J. Pringle. 1991. Use of a screen for synthetic lethal and multicopy suppressor mutants to identify two new genes involved in morphogenesis in *Saccharomyces cerevisiae*. *Mol. Cell. Biol.* 11:1295–1305.

Bogerd, A. M., J. A. Hoffman, D. C. Amberg, G. R. Fink, and L. I. Davis. 1994. *nup1* mutants exhibit pleiotropic defects in nuclear pore complex function. *J. Cell Biol.* 127:319–332.

Brandriss, M. 1987. Evidence for positive regulation of the proline utilization pathway in *Saccharomyces cerevisiae*. *Genetics.* 117:429–435.

Brewster, J. L., T. de Valoir, N. D. Dwyer, E. Winter, and M. C. Gustin. 1993. An osmosensing signal transduction pathway in yeast. *Science (Wash. DC).* 259:1760–1763.

Buss, F., and M. Stewart. 1995. Macromolecular interactions in the nucleoporin p62 complex of rat nuclear pores: binding of nucleoporin p54 to the rod domain of p62. *J. Cell Biol.* 128:251–261.

Chowdhury, S., K. W. Smith, and M. Gustin. 1992. Osmotic stress and the yeast cytoskeleton: phenotype-specific suppression of an actin mutation. *J. Cell Biol.* 118:561–571.

Copeland, C. S., and M. Snyder. 1993. Nuclear pore complex antigens delineate nuclear envelope dynamics in vegetative and conjugating *Saccharomyces cerevisiae*. *Yeast.* 9:235–249.

Costigan, C., S. Gehrung, and M. Snyder. 1992. A synthetic lethal screen identifies SLK1, a novel protein kinase homolog implicated in yeast cell morpho-

genesis and cell growth. *Mol. Cell. Biol.* 12:1162–1178.
Davis, L. I. 1995. The nuclear pore complex. *Annu. Rev. Biochem.* 64:865–896.
Davis, L. I., and G. Blobel. 1986. Identification and characterization of a nuclear pore complex protein. *Cell.* 45:699–709.
Davis, L. I., and G. R. Fink. 1990. The NUP1 gene encodes an essential component of the yeast nuclear pore complex. *Cell.* 61:965–978.
Doye, V., and E. C. Hurt. 1995. Genetic approaches to nuclear pore structure and function. *Trends Genet.* 11:235–241.
Doye, V., R. Wepf, and E. C. Hurt. 1994. A novel nuclear pore protein Nup133p with distinct roles in poly(A)+ RNA transport and nuclear pore distribution. *EMBO J.* 13:6062–6075.
Dujon, B., D. Alexandraki, B. Andre, W. Ansorge, V. Baladron, J. P. Ballestra, A. Banrerі, P. A. Bolle, M. Bolotin-Fukuhara, P. Bossier, et al. 1994. Complete DNA sequence of yeast chromosome XI. *Nature (Lond.).* 369:371–378.
Edgley, M., and A. D. Brown. 1983. Yeast water relations: physiological changes induced by solute stress in *Saccharomyces cerevisiae* and *Saccharomyces rouxii. J. Gen. Microbiol.* 129:3453–3463.
Fabre, E., W. C. Boelens, C. Wimmer, I. W. Mattaj, and E. C. Hurt. 1994. Nup145p is required for nuclear export of mRNA and binds homopolymeric RNA in vitro via a novel conserved motif. *Cell.* 78:275–289.
Featherstone, C., M. K. Darby, and L. Gerace. 1988. A monoclonal antibody against the nuclear pore complex inhibits nucleocytoplasmic transport of protein and RNA in vivo. *J. Cell Biol.* 107:1289–1287.
Finlay, D. R., E. Meier, P. Bradley, J. Jorecka, and D. J. Forbes. 1991. A complex of nuclear pore proteins required for pore function. *J. Cell Biol.* 114: 169–183.
Forrester, W., F. Stutz, M. Rosbash, and M. Wickens. 1992. Defects in mRNA 3′-end formation, transcription initiation, and mRNA transport associated with the yeast mutation prp20: possible coupling of mRNA processing and chromatin structure. *Genes & Dev.* 6:1914–1926.
Gietz, R. D., and A. Sugino. 1988. New yeast: *Escherischia coli* shuttle vectors constructed with *in vitro* mutagenized yeast genes lacking six-base pair restriction sites. *Gene.* 74:527–534.
Goldberg, M. W., and T. D. Allen. 1992. High resolution scanning electron microscopy of the nuclear envelope: the baskets of the nucleoplasmic face of the nuclear pores. *J. Cell Biol.* 119:1429–1440.
Gorsch, L. C., T. C. Dockendorff, and C. N. Cole. 1995. A conditional allele of the novel repeat-containing yeast nucleoporin *RAT7 / NUP159* causes both rapid cessation of mRNA export and reversible clustering of nuclear pore complexes. *J. Cell Biol.* 129:939–955.
Grandi, P., V. Doye, and E. C. Hurt. 1993. Purification of NSP1 reveals complex formation with "GLFG" nucleoporins and a novel nuclear pore protein NIC96. *EMBO J.* 12:3061–3071.
Grandi, P., S. Emig, C. Weise, F. Hucho, T. Pohl, and E. C. Hurt. 1995*a*. A novel nuclear pore protein Nup82p which specifically binds to a fraction of Nsp1p. *J. Cell Biol.* 130:1263–1273.
Grandi, P., N. Schlaich, H. Tekotte, and E. C. Hurt. 1995*b*. Functional interaction of Nic96p with a core nucleoporin complex consisting of Nsp1p, Nup49p and a novel protein Nup57p. *EMBO J.* 14:76–87.
Hinshaw, J. E., B. O. Carragher, and R. A. Milligan. 1992. Architecture and design of the nuclear pore complex. *Cell.* 69:1133–1141.
Hurwitz, M. E., and G. Blobel. 1995. NUP82 is an essential yeast nucleoporin required for poly(A)+ RNA export. *J. Cell Biol.* 130:1275–1281.
Jarnik, M., and U. Aebi. 1991. Toward a more complete 3-D structure of the nuclear pore complex. *J. Struct. Biol.* 107:291–308.
Kadowaki, T., Y. Zhao, and A. M. Tartakoff. 1992. A conditional yeast mutant deficient in mRNA transport from nucleus to cytoplasm. *Proc. Natl. Acad. Sci. USA.* 89:2312–2316.
Kadowaki, T., S. Chen, M. Hitomi, E. Jacobs, C. Kumagai, S. Liang, R. Schneiter, D. Singleton, J. Wisniewska, and A. M. Tartakoff. 1994. Isolation and characterization of Saccharomyces cerevisiae mRNA transport-defective (mtr) mutants. *J. Cell Biol.* 126:649–659.
Kraemer, D., R. W. Wozniak, G. Blobel, and A. Radu. 1994. The human CAN protein, a putative oncogene product associated with myeloid leukemogenesis, is a nuclear pore complex protein that faces the cytoplasm. *Proc. Natl. Acad. Sci. USA.* 91:1519–1523.
Kraemer, D. M., C. Strambio-de-Castillia, G. Blobel, and M. P. Rout. 1995. The essential yeast nucleoporin NUP159 is located on the cytoplasmic side of the nuclear pore complex and serves in karyopherin-mediated binding of transport substrate. *J. Biol. Chem.* 270:19017–19021.
Li, O., C. V. Heath, D. C. Amberg, T. C. Dockendorff, C. S. Copeland, M. Snyder, and C. N. Cole. 1995. Mutation or deletion of the *Saccharomyces cerevisiae RAT3/NUP133* gene causes temperature-dependent nuclear accumulation of poly(A)$^+$ RNA and constitutive clustering of nuclear pore complexes. *Mol. Biol. Cell.* 6:401–417.
Loeb, J., L. I. Davis, and G. R. Fink. 1993. NUP2, a novel yeast nucleoporin, has functional overlap with other proteins of the nuclear pore complex. *Mol. Biol. Cell.* 4:209–222.
Lupas, A., M. Can Dyke, and M. Stock. 1991. Predicting coiled coils from protein sequences. *Science (Wash. DC).* 252:1162–1164.
Maul, G. G. 1977. The nuclear and cytoplasmic pore complex: structure, dynamics, distribution and evolution. *Int. Rev. Cytol. Suppl.* 6:75–186.
Megnet, R. 1966. Osmotic remedial and osmotic sensitive mutants of *Schizosaccharomyces pombe. Experientia.* 22:216–218.
Melchior, F., B. Paschal, J. Evans, and L. Gerace. 1993. Inhibition of nuclear protein import by nonhydrolyzable analogues of GTP and identification of the small GTPase Ran/TC4 as an essential transport factor. *J. Cell Biol.* 123: 1649–1659.
Metzenberg, R. L. 1968. Repair of multiple defects of a regulatory mutant of *Neurospora* by high osmotic pressure and by reversion. *Arch. Biochem. Biophys.* 125:532–541.
Mirzayan, C., C. S. Copeland, and M. Snyder. 1992. The NUF1 gene encodes an essential coiled-coil related protein that is a potential component of the yeast nucleoskeleton. *J. Cell Biol.* 116:1319–1332.
Moore, M. S., and G. Blobel. 1993. The GTP-binding protein Ran/TC4 is required for protein import into the nucleus. *Nature (Lond.).* 365:661–663.
Moreland, R. B., G. L. Langevin, R. H. Singer, R. L. Garcea, and L. M. Hereford. 1987. Amino acid sequences that determine the nuclear localization of yeast histone 2B. *Mol. Cell. Biol.* 7:4048–4057.
Mortimer, R., C. Contopoulou, and J. King. 1992. Genetic and physical maps of *Saccharomyces cerevisiae.* Edition 11. *Yeast.* 8:817–902.
Nehrbass, U., H. Kern, A. Mutvei, H. Horstmann, B. Marshallsay, and E. C. Hurt. 1990. NSP1: a yeast nuclear envelope protein localized at the nuclear pores exerts its essential function by its carboxy-terminal domain. *Cell.* 61: 979–989.
Panté, N., R. Bastos, I. McMorrow, B. Burke, and U. Aebi. 1994. Interactions and three-dimensional localization of a group of nuclear pore complex proteins. *J. Cell Biol.* 126:603–617.
Park, M. K., M. D'Onofrio, M. C. Willingham, and J. A. Hanover. 1987. A monoclonal antibody against a family of nuclear pore proteins (nucleoporins): O-linked *N*-acetylglucosamine is part of the immunodeterminant. *Proc. Natl. Acad. Sci. USA.* 84:6462–6466.
Pemberton, L. F., M. P. Rout, and G. Blobel. 1995. Disruption of the nucleoporin gene NUP133 results in clustering of nuclear pore complexes. *Proc. Natl. Acad. Sci. USA.* 92:1187–1191.
Powers, M. A., C. Macaulay, F. R. Masiarz, and D. J. Forbes. 1995. Reconstituted nuclei depleted of a vertebrate GLFG nuclear pore protein, p97. *J. Cell Biol.* 128:721–736.
Radu, A., M. S. Moore, and G. Blobel. 1995. The peptide repeat domain of the nucleoporin Nup98 functions as a docking site in transport across the nuclear pore complex. *Cell.* 81:215–222.
Rasmussen, S. 1994. Sequence of a 28.6 kb region of yeast chromosome XI includes the FBA1 and TOA2 genes, an open reading frame (ORF) similar to a translationally controlled tumour protein, one ORF containing motifs also found in plant storage proteins and 13 ORFs with weak or no homology to known proteins. *Yeast.* 10(Suppl. A):S63–68.
Reed, R. H., J. A. Chudek, R. Foster, and G. M. Gadd. 1987. Osmotic significance of glycerol accumulation in exponentially growing yeasts. *Appl. Environ. Micro.* 53:2119–2123.
Reichelt, R., A. Holzenburg, E. L. Buhle, Jr., M. Jarnik, A. Engel, and U. Aebi. 1990. Correlation between structure and mass distribution of the nuclear pore complex and of distinct pore complex components. *J. Cell Biol.* 110: 883–894.
Ren, M., G. Drivas, P. D'Eustachio, and M. G. Rush. 1993. RAN/TC4: a small nuclear GTP-binding protein that regulates DNA synthesis. *J. Cell Biol.* 120: 313–323.
Richardson, W. D., A. D. Mills, S. M. Dilworth, R. A. Laskey, and C. Dingwall. 1988. Nuclear protein migration involves two steps: rapid binding at the nuclear envelope followed by slower translocation through nuclear pores. *Cell.* 52:655–664.
Riles, L., J. E. Dutchik, A. Baktha, B. K. McCauley, E. C. Thayer, M. P. Leckie, V. V. Braden, J. E. Depke, and M. V. Olson. 1993. Physical maps of the six smallest chromosomes of *Saccharomyces cerevisiae* at a resolution of 2.6 kilobase pairs. *Genetics.* 134:81–150.
Ris, H., and M. Malecki. 1993. High-resolution field emission scanning electron microscope imaging of internal cell structures after Epon extraction from sections: a new approach to correlative ultrastructural and immunocytochemical studies. *J. Struct. Biol.* 111:148–157.
Rose, M. D., F. Winston, and P. Hieter. 1989. Methods In Yeast Genetics. Cold Spring Harbor Laboratory, Cold Spring Harbor, NY.
Rout, M. P., and G. Blobel. 1993. Isolation of the yeast nuclear pore complex. *J. Cell Biol.* 123:771–783.
Rout, M. P., and S. R. Wente. 1994. Pores for thought: nuclear pore complex proteins. *Trends Cell Biol.* 4:357–365.
Schlenstedt, G., C. Saavedra, J. D. J. Loeb, C. N. Cole, and P. A. Silver. 1995. The GTP-bound form of the yeast Ran/TC4 homologue blocks nuclear protein import and appearance of poly (A)+ RNA in the cytoplasm. *Proc. Natl. Acad. Sci. USA.* 92:225–229.
Severs, N. J., E. G. Jordan, and D. H. Williamson. 1976. Nuclear pore absence from areas of close association between nucleus and vacuole in synchronous yeast cultures. *J. Ultrastruct. Res.* 54:374–387.
Sherman, F. 1991. Getting started with yeast. *Methods Enzymol.* 194:3–21.
Snow, C. M., A. Senior, and L. Gerace. 1987. Monoclonal antibodies identify a group of nuclear pore complex glycoproteins. *J. Cell Biol.* 104:1143–1156.
Stewart, M., and S. Whytock. 1988. The structure and interactions of components of nuclear envelopes from Xenopus oocyte germinal vesicles observed by heavy metal shadowing. *J. Cell Sci.* 90:409–423.
Tollervey, D., and I. W. Mattaj. 1987. Fungal small nuclear ribonucleoproteins share properties with plant and vertebrate U-snRNPs. *EMBO J.* 6:469–476.
Traglia, H. M., N. S. Atkinson, and A. K. Hopper. 1989. Structural and func-

tional analysis of *Saccharomyces cerevisiae* wild-type and mutant RNA1 genes. *Mol. Cell. Biol.* 9:2989–2999.

Udem, S. A., and J. R. Warner. 1973. The cytoplasmic maturation of a ribosomal precursor RNA in yeast. *J. Biol. Chem.* 248:1412–1416.

Unwin, P. N., and R. A. Milligan. 1982. A large particle associated with the perimeter of the nuclear pore complex. *J. Cell Biol.* 93:63–75.

Varela, J. C., C. van Beekvelt, R. J. Planta, and W. H. Mager. 1992. Osmostress induced changes in Yeast gene expression. *Mol. Microbiol.* 6:2183–2190.

Wente, S. R., and G. Blobel. 1993. A temperature-sensitive *NUP116* null mutant forms a nuclear envelope seal over the yeast nuclear pore complex thereby blocking nucleocytoplasmic traffic. *J. Cell Biol.* 123:275–284.

Wente, S. R., and G. Blobel. 1994. *NUP145* encodes a novel yeast glycine-leucine-phenylalanine-glycine (GLFG) nucleoporin required for nuclear envelope structure. *J. Cell Biol.* 125:955–969.

Wente, S. R., M. P. Rout, and G. Blobel. 1992. A new family of yeast nuclear pore complex proteins. *J. Cell Biol.* 119:705–723.

Wimmer, C., V. Doye, P. Grandi, U. Nehrbass, and E. C. Hurt. 1992. A new subclass of nucleoporins that functionally interact with nuclear pore protein NSP1. *EMBO J.* 11:5051–5061.

Wozniak, R. W., G. Blobel, and M. P. Rout. 1994. POM152 is an integral protein of the pore membrane domain of the yeast nuclear envelope. *J. Cell Biol.* 125:31–42.